Linköping Studies in Science and Technology
Thesis No. 1319

Look-ahead Control of Heavy Trucks utilizing Road Topography

Erik Hellström

Linköpings universitet
INSTITUTE OF TECHNOLOGY

Department of Electrical Engineering
Linköpings universitet, SE–581 83 Linköping, Sweden

Linköping 2007

Look-ahead Control of Heavy Trucks utilizing Road Topography

hellstrom@isy.liu.se
http://www.vehicular.isy.liu.se
Department of Electrical Engineering,
Linköpings universitet,
SE–581 83 Linköping,
Sweden.

ISBN 978-91-85831-58-6
ISSN 0280-7971
LIU-TEK-LIC-2007:28

Printed by LiU-Tryck, Linköping, Sweden 2007

Abstract

The power to mass ratio of a heavy truck causes even moderate slopes to have a significant influence on the motion. The velocity will inevitable vary within an interval that is primarily determined by the ratio and the road topography. If further variations are actuated by a controller, there is a potential to lower the fuel consumption by taking the upcoming topography into account. This possibility is explored through theoretical and simulation studies as well as experiments in this work.

Look-ahead control is a predictive strategy that repeatedly solves an optimization problem online by means of a tailored dynamic programming algorithm. The scenario in this work is a drive mission for a heavy diesel truck where the route is known. It is assumed that there is road data on-board and that the current heading is known. A look-ahead controller is then developed to minimize fuel consumption and trip time.

The look-ahead control is realized and evaluated in a demonstrator vehicle and further studied in simulations. In the prototype demonstration, information about the road slope ahead is extracted from an on-board database in combination with a GPS unit. The algorithm calculates the optimal velocity trajectory online and feeds the conventional cruise controller with new set points. The results from the experiments and simulations confirm that look-ahead control reduces the fuel consumption without increasing the travel time. Also, the number of gear shifts is reduced. Drivers and passengers that have participated in tests and demonstrations have perceived the vehicle behavior as comfortable and natural.

Acknowledgments

This work has been carried out at the division of Vehicular Systems, department of Electrical Engineering, Linköpings universitet in Sweden. First of all, I would like to express my gratitude to my supervisor Professor Lars Nielsen for letting my join the group and for all of his work and encouragement during the project.

A sincere appreciation is due to to my friend and second supervisor Jan Åslund for ideas and discussions regarding the work. Erik Frisk is a good friend who also aided with the layout of the thesis. Anders Fröberg was a dedicated supervisor during my Master's thesis project and is now a valuable colleague and friend. Carolina Fröberg is always sparkling and takes care of administrative tasks. Everyone at the division is finally thanked for jointly creating a positive and nice atmosphere to work in.

I am indebted to a number of people at SCANIA who made the experiments possible. Maria Ivarsson put in a lot of work when we collaborated to realize the control algorithm and performed trials and demonstrations. Per Sahlholm, Anders Jensen and Nils-Gunnar Vågstedt are further appreciated for their efforts.

The work has been funded by the Swedish Foundation for Strategic Research SSF through the research center MOVIII. The support is gratefully acknowledged.

My love goes to my family, my friends and Gabriella.

Erik Hellström
Linköping, May 2007

Contents

1

Introduction

About 30% of the life cycle cost of a heavy diesel truck comes from fuel expenses. This cost is, besides salaries, the largest individual share of the total cost for a truck owner. Further, the average mileage for a European heavy truck is 150,000 km per year and the average fuel consumption is 32.5 L/100km (Schittler, 2003). One percent of the consumed fuel volume per year is, with these average numbers, almost 500 liters. Lowering the consumption with a couple of percent will thus translate into significant cost reductions with the current, and predicted future, prices of fuel. These reasons make it appealing to owners and manufacturers of heavy trucks to aim at reduced fuel consumption.

The term *heavy truck* is here used to denote a class 8 truck, that is a truck with a gross vehicle weight above 16 tonnes. The focus is on heavy trucks used for long-haulage. The power to mass ratio of these vehicles is often such that even moderate slopes have significant influence on the motion. The truck will then accelerate in downhills without engine propulsion and decelerate in uphills despite maximum engine power. The velocity will thus vary within an interval determined by the available power and the present road topography. These variations are inevitable. If additional variations are allowed to be actuated by a controller there is a potential to select control actions with respect to the upcoming topography with the aim to reduce the fuel consumption. This possibility will be explored through both theoretical and simulation studies as well as experiments in this work.

Look-ahead control is a predictive control strategy where information about some of the future disturbances to the controlled system is assumed to be available. In this work the additional knowledge includes the road topography ahead

of the vehicle and the aim is to utilize this information for reducing the fuel consumption. Figure 1.1 depicts a visionary scenario of look-ahead control. A control unit consisting of several modules represents a complex decision system. The unit receives information about the current position with aid of a satellite navigation system and it is also able to receive various information by telemetry and there is a ranging sensor that measures distance to other vehicles. On-board databases with altitude and curvature information are also present. The task of the decision system is to take advantage of the available information to achieve set objectives.

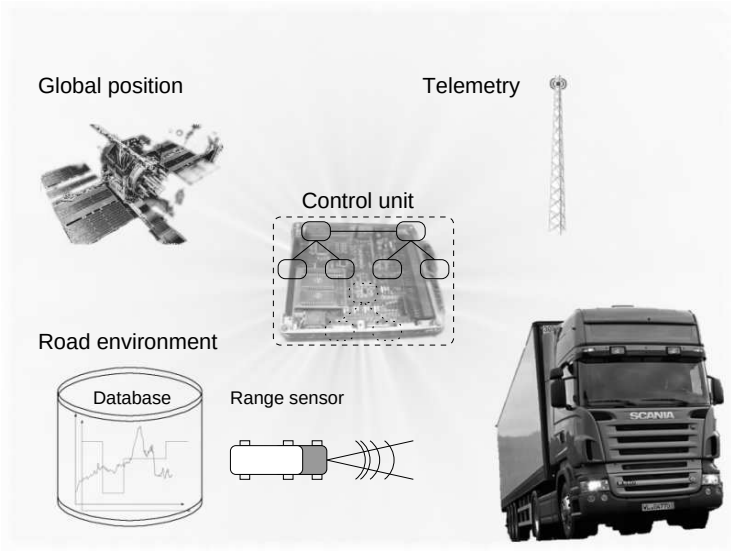

Figure 1.1: Visionary scenario of look-ahead control.

1.1 Outline and Contributions

The chain of steps in the thesis and the corresponding chapters are shown in Figure 1.2. The scenario that is considered in the thesis is first defined in Chapter 2 and related work is surveyed. The look-ahead control strategy is described. On the basis of the formulated scenario, a longitudinal vehicle model is developed in Chapter 3 that captures the important features. Criteria are devised that reflects the objective of minimizing the fuel consumption for a given drive mission.

The look-ahead control strategy entails a dynamic programing algorithm that is presented in Chapter 5. The theory and computational aspects of dynamic programming are therefore treated ahead in Chapter 4.

The setup for simulations and experiments are explained in Chapter 6. Then,

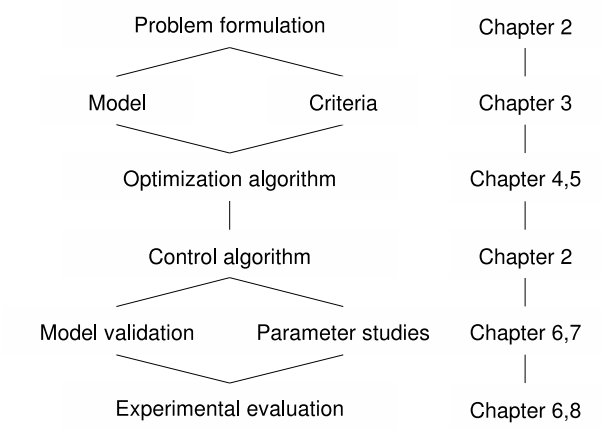

Figure 1.2: The outline excluding introductory and concluding chapters.

the prediction model is validated and a number of parameter studies are undertaken in Chapter 7. The control algorithm is finally evaluated in experiments reported in Chapter 8. The work finishes with conclusions in Chapter 9.

The thesis builds upon both published and previously unpublished work. The basic development of the control algorithm is reported in

> Hellström, E., Fröberg, A., and Nielsen, L. (2006). A real-time fuel-optimal cruise controller for heavy trucks using road topography information. Number 2006-01-0008 in SAE World Congress, Detroit, MI, USA.

An improved approach with evaluation in real trial runs are reported in

> Hellström, E., Ivarsson, M., Åslund, J., and Nielsen, L. (2007). Look-ahead control for heavy trucks to minimize trip time and fuel consumption. 5th IFAC Symposium on Advances in Automotive Control, Monterey, CA, USA.

2

Look-ahead Control

The scenario studied in the thesis is defined first in this chapter. Distinguishing aspects of the problem are identified and related work is surveyed. A study of a simplified problem is undertaken to gain basic insights into the nature of the present challenge. Finally, the look-ahead control strategy is formulated.

2.1 Scenario

The considered situation is a drive mission for a heavy truck where the route is known. It is not assumed that the vehicle constantly operates on the same route. Instead, it is envisioned that there is road data on-board and that the current heading is known. This look-ahead information includes a database with altitude information that is used in combination with a global positioning system. The road information may be stored on-board, recorded on-line or even transmitted from other trucks in a fleet. The current heading may be supplied by the driver or be predicted by assigning probabilities to possible future route choices presuming an on-board map.

It is assumed that a model exists to enable prediction of vehicle motion and energy consumption as a function of control signals and known disturbances. The control signals that are supposed to be available are fueling level, brake level and gear ratio selection. The road slope can be obtained from the altitude information and is thus a known disturbance.

2.1.1 Objectives

A drive mission is given by a route, an allowed velocity range and a desired maximum trip time. The route is defined by its latitudinal and longitudinal coordinates. The allowed velocities will be constrained to a set that is determined by e.g. the acceptable trip time in combination with legal and safety considerations.

The objective is to minimize the fuel energy required for a given mission. The purpose of the control is to take advantage of the look-ahead information in order to actuate fuel-optimal velocity trajectories and gear shifting schemes.

2.1.2 Key Features

A model of vehicle motion normally has a continuous character. However, the inclusion of gear selection in the set of control signals is distinguishing since it introduces a discrete nature in the model. A dynamic model including the transmission is thus of hybrid nature, that is a model containing both continuous and discrete components.

The aim is ultimately an optimizing controller that works on-board in a real environment. This has several implications. It limits the available computational power. Further, the technique must be robust against present disturbances and cooperate well with the driver and on-board controllers.

2.2 Related Work

This section will survey related work from different categories but starts with the work closest to the current application.

Predictive control algorithms and computer simulation results for vehicles where an on-board map of the road geometry is utilized are reported in a number of conference papers stemming from DaimlerChrysler (Back et al., 2002; Kirschbaum et al., 2002; Back et al., 2004; Finkeldei and Back, 2004; Terwen et al., 2004; Jonsson and Jansson, 2004; Lattemann et al., 2004) and the thesis Back (2006). These works deal with automobiles, trucks as well as hybrid electric vehicles. The results are mostly limited to computer simulations. The thesis Back (2006) and the paper Finkeldei and Back (2004), which are focused on hybrid electric vehicles, contain experimental results as well as simulation results. A related patent application is Neiss et al. (2004). Dynamic programming is used in the automobile and hybrid vehicle applications whereas a combination of combinatorial search and a shooting algorithm is used in the truck applications.

In Bemporad and Morari (1999) a modeling framework is proposed for systems described by linear dynamic equations and linear inequalities containing real and integer variables. For quadratic criteria, a predictive control scheme is presented that uses mixed integer quadratic programming for optimization. Applications in the automotive field that stem from this framework are reported in e.g. Borrelli et al. (2006); Giorgetti et al. (2006a,b).

Control strategies for hybrid electrical vehicles bear similarities to the scenario in the present work. Optimization of such systems and references to earlier work are given in Guzzella and Sciarretta (2005).

In Hellström et al. (2006) a predictive cruise controller is developed for a heavy truck where dynamic programming is used to numerically solve the optimal control problem. Hellström et al. (2007) is a continuation where an improved approach is realized and evaluated in real trial runs and not only in a simulation environment.

2.2.1 Optimal Control

One early work (Schwarzkopf and Leipnik, 1977) formulates an optimal control problem for a nonlinear vehicle model with the aim to minimize fuel consumption. The model entailed quadratic polynomials for the power output and energy consumption of the vehicle. A varying road slope together with the controls, engine power and gear ratio, make up the inputs. Explicit solutions were obtained for constant road slopes. Hooker et al. (1983); Hooker (1988) are continuations where the polynomial models are replaced with piecewise quadratic surfaces that are fitted to measurement data. A forward dynamic programming technique gives numerical solutions to different problem scenarios. The controls were acceleration and gear ratio and the model states were traveled distance, velocity and current gear. A dynamic programming approach is also taken in Monastyrsky and Golownykh (1993) but the problem is formulated as dependent on distance rather than time. The travel time is included in the objective function combined with the fuel consumption. Through this only velocity and current gear need to be considered as states which gave a decreased computation time required for a solution. Inspired of some of the results indicated in these and other works it was shown in Chang and Morlok (2005); Fröberg et al. (2006) with varying vehicle model complexity, that constant speed is optimal within certain bounds on the road slope. The result relies on the assumption that the fuel consumption is an affine function of the produced work. The road slope should be such that the constant speed level can be maintained in uphills and such that braking is not needed in downhills.

A study of the situation when the relation between power output and energy consumption is nonlinear is made in Fröberg and Nielsen (2007). Using piecewise affine models the analysis of optimal control for fuel minimization is kept in an analytical framework.

2.2.2 Train Applications

The problem of optimal control for energy minimization of rail vehicles poses similar challenges as the study of road vehicles. In these train problems the motion resistance is highly dependent on the road slope and hence it is not reasonably to neglect variations of the slope along the route of travel. One interesting work along with references to earlier work in the same field are

given in Liu and Golovitcher (2003). In the model used there is one continuous control variable and it determines the traction force. The main results are the identification of the set of optimal controls and the conditions that determines the optimal sequence of these. If a constant transmission ratio is assumed, the model that is used correspond to a simple longitudinal vehicle model and the results are directly applicable. In other train applications the available controls are a set of constant fuel supply rates. The results in Howlett (1996) state that certain key equations gives necessary conditions for optimal strategies. The result relies on a linear relationship between fuel rate and power output.

2.2.3 Auxiliary Units and Neutral Gear

The contribution to the energy consumption in a heavy truck due to auxiliary units, such as a water pump or a cooling fan, has been investigated, see Pettersson and Johansson (2004) and references therein. Assuming that a unit is electrically driven, optimal control theory is applied to derive strategies for controlling some auxiliary devices. Computer simulations show that it is possible to reduce the energy consumption significantly.

Engaging neutral gear on the basis of road slope information is one approach to lower the fuel consumption. Neutral gear decouples the engine and the inertia and load of the rest of the powertrain are thereby lessened, since running the engine with zero fueling gives a drag torque. With the engine decoupled, idle speed must however generally be maintained which requires a non-zero fueling level. The trade off is clear; the motion resistance is lessened with neutral gear at the cost of idling and the required shifts. Computer simulation results have been reported that indicates that there is a possible potential (Fröberg et al., 2005; Hellström et al., 2006). The truck manufacturer VOLVO has also launched a transmission that utilizes neutral gear with the aim to improve fuel economy (Volvo press release, 2006).

2.3 A Basic Analysis

Consider the motion of a vehicle in one dimension, see Figure 2.1. The body is considered as a point mass and is acted upon by two forces, a driving force and a resisting force. The driving force is given by the function $g(u)$ where u is a scalar control variable. The resisting force is dependent on the position x and the velocity v and is denoted by the function $f(x, v)$. It is assumed that this function is monotonically increasing for $v > 0$, that is

$$\frac{\partial f}{\partial v} \geq 0, v > 0 \tag{2.1}$$

which should hold for any physically plausible resistance function. The problem of finding the velocity trajectory that minimizes the work required to move the vehicle from one point $x = 0$ to another point $x = s$ is now studied. A constraint

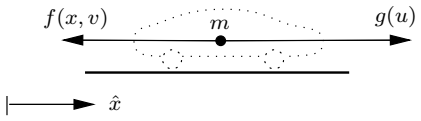

Figure 2.1: A vehicle moving in one dimension.

is set on the desired time for the trip and it is assumed that the velocity is positive at all times.

Newton second law of motion gives

$$m\frac{dv}{dt} = g(u) - f(x,v) \tag{2.2}$$

which governs the motion. Rewrite according to

$$\frac{dv}{dt} = \frac{dv}{dx}\frac{dx}{dt} = v\frac{dv}{dx} \tag{2.3}$$

in order to receive the model

$$mv\frac{dv}{dx} = g(u) - f(x,v). \tag{2.4}$$

The propulsive work equals

$$\begin{aligned} W &= \int_0^s g(u)dx = \int_0^s \left(mv\frac{dv}{dx} + f(x,v)\right) dx \\ &= \frac{m}{2}\left(v(s)^2 - v(0)^2\right) + \int_0^s f(x,v)\, dx \end{aligned} \tag{2.5}$$

that is, the sum of the difference in kinetic energy and the work due to the resisting force along the path.

The problem objective is now stated as

$$\min_{v(x)} \int_0^s \left(mv(x)\frac{dv(x)}{dx} + f(x,v(x))\right) dx \tag{2.6}$$

with the time constraint expressed as

$$\int_0^s \frac{dx}{v(x)} \leq T \tag{2.7}$$

where T denotes the desired maximum time.

If the inequality in (2.7) is replaced by an equality, the resulting problem is an isoperimetric problem. The core in the calculus of variations is the Euler equation, which for a functional $\int F(x,y,y')\, dx$ is

$$\frac{\partial F}{\partial y} - \frac{d}{dx}\frac{\partial F}{\partial y'} = 0. \tag{2.8}$$

If the functional has an extremum for a function $y(x)$ but this function does not yield the desired value of another functional $\int G(x, y, y')\, dx$, there exist a constant λ such that the Euler equation is satisfied for the functional $\int F + \lambda G\, dx$. (Gelfand and Fomin, 1963)

Only smooth solutions will be considered, so it is assumed that the studied functional has continuous first and second order derivatives in the considered interval for arbitrary v and v'.

In the present problem, the functional

$$\int_0^s (mv\frac{dv}{dx} + f(x, v) + \frac{\lambda}{v})\, dx \tag{2.9}$$

is formed, where λ is a constant. Then, according to the Euler equation

$$m\frac{dv}{dx} + \frac{\partial f}{\partial v} - \frac{d}{dx}(mv) + \lambda\left(-\frac{1}{v^2}\right) = 0 \tag{2.10}$$

should be satisfied which yields that

$$v^2\frac{\partial}{\partial v}f(x, v) = \lambda \tag{2.11}$$

is a necessary condition for the objective to have an extremum for a function $v(x)$. Due to the assumption (2.1), the multiplier λ will be positive. Relaxing the equality constraint to the inequality (2.7) does not alter the solution. Every $v(x)$ that becomes admissible when the equality constraint is replaced with an inequality will have a higher value of the objective (2.6) due to (2.1).

In order to proceed, assume that the resistance function is a sum of two functions with explicit dependency on x and v respectively, that is

$$f(x, v) = f_1(x) + f_2(v). \tag{2.12}$$

The condition (2.11) then becomes

$$v^2\frac{\partial}{\partial v}f_2(v) = \lambda. \tag{2.13}$$

For a given λ, the solution to (2.13) is constant velocity. To minimize the work for moving the body from one point to another point, the extremum is thus a constant speed level adjusted to match the desired trip time.

Common resisting force models fulfill (2.12). By using such explicit models results corresponding to (2.13) is obtained in different ways in Fröberg et al. (2006); Chang and Morlok (2005) where the fuel consumption is minimized. The consumption is however assumed to be a linear function of the produced work which makes the minimization equal to the objective used here. An analytical approach to a fuel minimization problem with a nonlinear mapping between work and fuel consumption is taken in e.g. Schwarzkopf and Leipnik (1977); Fröberg and Nielsen (2007).

2.3.1 Comparison with the Present Problem

For the illustrative problem depicted in Figure 2.1, constant speed is shown to be the solution to the problem of minimizing the needed work to move from one point to another with a trip time constraint. The assumptions are that the velocity and acceleration are smooth and that (2.1), (2.2) and (2.12) holds. If the fuel consumption is an affine function of the produced work, the solution is still constant velocity. However, it is not reasonable to expect that a heavy truck can keep a desired cruising speed on all road profiles. The ratio of available engine power to the vehicle mass makes a constant speed level inadmissible since it can not be realized. If the speed can not be kept constant it is not plausible that is it possible to always have the same gear engaged either. Including gear selection into the problem description renders an optimal control problem for a hybrid system which presently is a challenging task. With a large mass, the delay when shifting gears becomes significant. Taking this into account gives additional model complexity. If the assumption that there is an affine relationship between produced work and fuel consumption does not hold, the optimal velocity trajectory will in general be even more difficult to obtain.

2.4 Strategy

Model predictive control relies on a model and an objective function including predicted future performance of the controlled system (Levine, 1996; Camacho and Bordons, 2004). The control signals that optimize the objective are repeatedly calculated. The horizon over which the predictions are made is constantly moved forward allowing for new controls to be calculated.

Look-ahead control is a predictive control scheme with additional knowledge, look-ahead information, about some of the future disturbances to the controlled system. In the current application, this additional knowledge includes the road topography ahead of the vehicle. The information is included in a criterion that involves predicted future behavior of the system, and is then optimized by finding the proper control signals. The optimization will in this work be accomplished through discrete deterministic dynamic programming (DP). The theory and computational aspects of DP will therefore be treated in Chapter 4.

Let the discrete process model be described by

$$x_{k+1} = f_k(x_k, u_k)$$

where x_k, u_k denotes the state and control vectors. Divide the distance of the entire drive mission into M steps. The performance criterion over this horizon is then formulated as

$$\zeta_M(x_M) + \sum_{i=0}^{M-1} \zeta_i(x_i, u_i)$$

where ζ_i and ζ_M defines the running and the terminal cost respectively.

To obtain the discrete process model, the original problem is discretized. A look-ahead horizon is obtained by truncating the entire drive mission horizon of M steps to $N < M$ steps. This shorter horizon is used in the online optimization. Therefore, the criterion is rewritten as

$$\sum_{i=0}^{N-1} \zeta_i(x_i, u_i) + \zeta_M(x_M) + \sum_{i=N}^{M-1} \zeta_i(x_i, u_i)$$

and the last two terms are approximated by $\tilde{\zeta}_N(x_N)$. The approximation procedure is an important issue that can be dealt with in different ways, see e.g. Bertsekas (2005). The problem is now only defined over the look-ahead horizon and

$$\min_{u_0,\cdots,u_{N-1}} \tilde{\zeta}_N(x_N) + \sum_{i=0}^{N-1} \zeta_i(x_i, u_i)$$

is to be solved in each iteration. This method appears in dynamic programming literature under the name limited look-ahead policy. The control u_0 is applied to the system and the procedure restarts with new initial values and a horizon that has moved forward in order to calculate the next control.

An illustration is given in Figure 2.2. At point A, the optimal solution is sought for the problem that is defined over the look-ahead horizon. This horizon is obtained by truncating the entire drive mission horizon. Only the first optimal control is applied to the system and the procedure is repeated at point B.

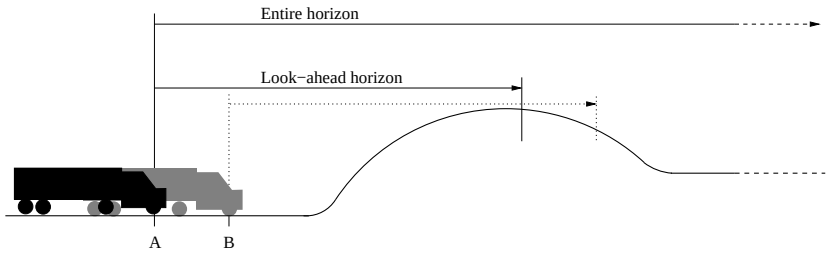

Figure 2.2: Illustration of the look-ahead control strategy.

3

Model and Criterion Formulation

In this chapter the models used will be described. They are built upon commonly used relationships based on the physical principles for the different components. Then, control criteria are devised on the basis of the models and the problem formulation.

3.1 Powertrain Modeling

The continuous and discrete components of the powertrain are described following standard modeling as in Kiencke and Nielsen (2005). The modeling has two purposes. First, a model is used to predict vehicle motion and energy consumption as a function of the road, state and control signals. Second, evaluation of algorithms by simulations requires a model for comparison. The main difference between the prediction and evaluation model is the modeling of the engine torque generation.

In the following the physical principles, on which the models of the respective component build upon, are described. A powertrain with some of its components labeled are depicted in Figure 3.1.

3.1.1 Engine

In a combustion engine, chemical processes take place that produces power and emissions from fuel and air. To model the power output, the produced torque from the reaction and the resulting engine revolution speed must be known. The formation of emissions is dependent on a number of complex reactions during

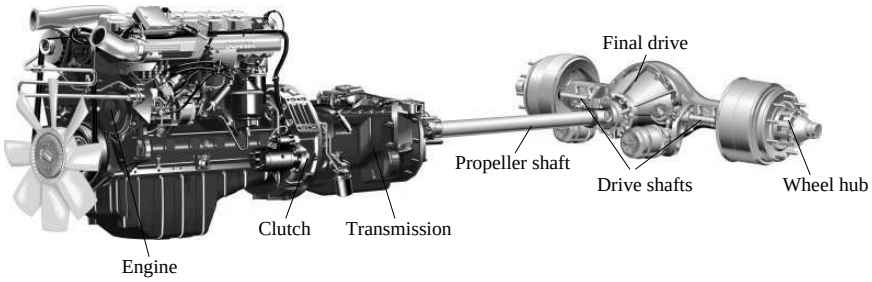

Figure 3.1: A powertrain.

the combustion. Modeling of the formation of emissions will not be dealt with since none of the objectives in the present work relate to emissions.

The useful torque T_e generated by the engine is related to the indicated gross energy produced in the combustion process and losses in the combustion chamber, such as friction and pumping work. The approach followed here is to model engine torque by assuming that it is merely dependent on the amount of fueling u_f and engine speed ω_e (Sandberg, 2001a),

$$T_e = f_e(\omega_e, u_f). \tag{3.1}$$

The engine revolution speed, ω_e, is determined by the torque output from the engine T_e and the load T_c from the driveline through the clutch. Given the inertia of the rotating parts J_e, Newton's second law of motion gives the governing dynamics for the engine speed,

$$J_e\dot{\omega}_e = T_e - T_c. \tag{3.2}$$

3.1.2 Transmission and Final Drive

It is assumed that the transmission is of the automated manual type. The transmission is commonly manual for heavy trucks due to cost, durability and efficiency in comparison with an automatic transmission (Pettersson, 1997).

The clutch transmits the engine torque to the transmission. In case of a powertrain with manual transmission, a friction clutch is used to decouple the engine during manual gear shifts. However, it is here assumed that gear shifts are accomplished through engine control without using the clutch. The clutch is thus assumed to be engaged at all times when the vehicle is not in a standstill.

The final drive transmits the torque from the propeller shaft to the drive shafts. If the drive shafts and the wheels are lumped into single components, the final drive is viewed as a transmission with a fixed ratio. It can then be modeled analogously to the transmission.

When a gear is engaged, a scaling of the input and output rotational speeds is achieved. If the ratio is denoted i and the input speed ω_i and the output

speed ω_o, the relation

$$\omega_i = i\omega_o \tag{3.3}$$

holds. Denote the input torque T_i and the output torque T_o. The dynamics for a transmission is then given by

$$J_t\omega_o = iT_i - T_o - T_f \tag{3.4}$$

where J_t is the transmission inertia and T_f is friction losses.

Friction losses are modeled as a torque T_f. A static efficiency η is a simple way to model this,

$$T_f = (1-\eta)iT_i. \tag{3.5}$$

3.1.3 Flexibilities and Backlash

There are backlash and oscillations in a vehicular driveline. Transmission components are the predominant source of backlash (Lagerberg and Egardt, 2007). The drive shafts are the components that generally have the largest flexibility and are the main cause of oscillations (Kiencke and Nielsen, 2005). These phenomena mainly impact driveability and not fuel consumption (Sandberg, 2001a) and will therefore be disregarded with the current purpose of the modeling.

3.1.4 Driveline Equations

The driveline is assumed stiff since flexibility and backlash are neglected. Friction losses in the transmission and the final drive are modeled with a lumped efficiency η. This allows for the driveline to be viewed as one lumped rotating inertia J_l. When a gear is engaged this gives using (3.3), (3.4) and (3.5),

$$\begin{aligned} \omega_e &= i\omega_w \\ T_w &= i\eta T_c \\ J_l\dot{\omega}_w &= T_w - T_b - r_w F_w \end{aligned} \tag{3.6}$$

where ω_w is the wheel speed, T_w is the torque transmitted to the wheel and r_w is the wheel radius. F_w is the resulting friction force at the wheel. The braking torque T_b is determined by a normalized brake level $u_b \in [0,1]$ and a maximum torque parameter k_b,

$$T_b(u_b) = k_b u_b. \tag{3.7}$$

When neutral gear is engaged, the engine transmits zero torque to the driveline and

$$T_c = T_w = 0 \tag{3.8}$$

holds. The ratio i and efficiency η of neutral gear are defined to be zero.

3.1.5 Gear Shifts

Gear shifts are assumed to be carried out by engine control. This can be accomplished with different approaches. The basic challenges are nevertheless the same. To engage neutral gear without using the clutch, the transmission should first be controlled to a state where no torque is transmitted. The engine torque should then be controlled to a state where the input and output revolution speeds of the transmission are synchronized when the new gear is engaged. (Pettersson and Nielsen, 2000)

A shift will be modeled by a constant period of time τ_{shift} where the neutral gear is engaged before the new gear is engaged. The number of the currently engaged gear will be denoted g. The ratio i and efficiency η then becomes functions of g. The control signal that selects gear will be denoted u_g. Assume that u_g changes value from g_1 to g_2 at $t = 0$ and thereby commands a shift. The currently engaged gear $g(t)$ will then be described by

$$g(t) = \begin{cases} g_1 & , \quad t < 0 \\ 0 & , \quad 0 \leq t \leq \tau_{shift} \\ g_2 & , \quad t > \tau_{shift} \end{cases} \tag{3.9}$$

where gear zero corresponds to neutral gear.

3.1.6 Resisting Forces

In the vehicle longitudinal direction, the main resisting forces are considered to be air drag, rolling resistance and the gravitational force (Wong, 2001; Gillespie, 1992).

Air drag F_a is commonly estimated by

$$F_a = \frac{1}{2} c_w A_a \rho_a v^2 \tag{3.10}$$

where c_w is the air drag coefficient, A_a is the cross section area of the vehicle, ρ_a is the air density and v is the velocity of the vehicle relative to the wind.

In the literature, there exists many empirical formulas for the rolling resistance. They usually entails the tire normal force F_N multiplied with a rolling resistance coefficient c_r. The coefficient is often dependent on velocity but sometimes also on tire pressure and temperature. A model for the resistance is then

$$F_r = c_r F_N = c_r m g_0 \cos\alpha \tag{3.11}$$

where g_0 is the acceleration of gravity, α is the road slope and m is the vehicle mass. The coefficient c_r is here assumed constant in the evaluation and prediction models.

The resistance due to gravity is the longitudinal component F_l of the gravitational force. It is dependent on the road slope α and the mass of the vehicle m,

$$F_l = m g_0 \sin\alpha. \tag{3.12}$$

3.1.7 Wheels

The traction force developed at tire-ground contact patch mainly depends on the longitudinal slip. If the lateral slip is assumed low, the situation of pure longitudinal slip can be used for the sake of simplicity. Longitudinal slip s is commonly defined as

$$s = \frac{r_w\omega_w - v}{r_w\omega_w} \text{ or } s = \frac{r_w\omega_w - v}{v} \tag{3.13}$$

where r_w is the wheel radius, v is vehicle velocity and ω_w is the wheel speed of revolution. The longitudinal force depends nonlinearly on the slip s. (Wong, 2001; Pacejka, 2002)

The tire dynamics will be neglected and a rolling condition is assumed,

$$v = r_e\omega_w \tag{3.14}$$

which statically relates tire rotation ω_w and vehicle speed v through an effective radius r_e. Using (3.13), it is seen that this corresponds to a situation of a constant slip level.

3.1.8 Vehicle Motion

The vehicle motion in the longitudinal direction is modeled. The governing dynamics for the velocity v is

$$m\frac{dv}{dt} = F_w - F_a(v) - F_r(\alpha) - F_l(\alpha) \tag{3.15}$$

where α is the road slope.

3.1.9 Fuel Consumption

The mass flow of fuel $\dot{m}$ is determined by the fueling level u_f [g/cycle] and the engine speed ω_e [rad/s]. The mass flow in [g/s] is then

$$\dot{m}(\omega_e, u_f) = \frac{n_{cyl}}{2\pi n_r}\omega_e u_f \tag{3.16}$$

where n_{cyl} is the number of cylinders and n_r is the number of crankshaft revolutions per cycle. When neutral gear is engaged, the fuel flow is assumed constant and

$$\dot{m} = \dot{m}_{idle} \tag{3.17}$$

where $\dot{m}_{idle}$ is the idle fuel flow. The fuel consumption is then simply the integral of the flow.

3.1.10 Combined Equations

Combining the governing equations for the engine (3.2) and driveline dynamics (3.6), using the rolling condition (3.14) and inserting into the motion equation (3.15) gives

$$\frac{dv}{dt} = \frac{r_w}{J_l + mr_w^2 + \eta i^2 J_e}\Big(i\eta T_e(v, u_f) - T_b(u_b) - r_w\left(F_a(v) + F_r(\alpha) + F_l(\alpha)\right)\Big) \tag{3.18}$$

when a gear is engaged. In case of neutral gear, using Equation (3.8) in the equations for the engine and driveline dynamics gives

$$\frac{dv}{dt} = \frac{r_w}{J_l + mr_w^2}\left(-T_b(u_b) - r_w\left(F_a(v) + F_r(\alpha) + F_l(\alpha)\right)\right). \tag{3.19}$$

The gear ratio $i(g)$ and efficiency $\eta(g)$ are functions of the engaged gear number, denoted g. Neutral gear gives $i(0) = \eta(0) = 0$. Equations (3.18) and (3.19) can now finally be written as

$$\frac{dv}{dt}(x, u, \alpha) = \frac{r_w}{J_l + mr_w^2 + \eta(g)i(g)^2 J_e}\Big(i(g)\eta(g)T_e(v, u_f) - T_b(u_b) - r_w\left(F_a(v) + F_r(\alpha) + F_l(\alpha)\right)\Big) \tag{3.20}$$

where

$$x = [v, g]^T \quad u = [u_f, u_b, u_g]^T \tag{3.21}$$

denote the state and control vector respectively. The states are the velocity v and currently engaged gear g and the controls are fueling u_f, braking u_b and gear u_g. In case of a gear shift, Equation (3.9) describes the currently engaged gear g.

Using (3.6) and (3.14) together with (3.16) and (3.17) gives the fuel flow

$$\dot{m}(x, u) = \begin{cases} \frac{n_{cyl}}{2\pi n_r}\frac{i(g)}{r_w} v u_f, & g \neq 0 \\ \dot{m}_{idle}, & g = 0 \end{cases} \tag{3.22}$$

where u_g and g denotes the gear control and state respectively. The fuel consumption for an interval $[t_0, t_f]$ is then given by

$$\int_{t_0}^{t_f} \dot{m}(x, u)\, dt. \tag{3.23}$$

3.1.11 Prediction Model

The powertrain dynamics are given by (3.20) with resisting forces according to (3.10) to (3.12). The engine torque (3.1) will in the prediction model be

modeled as a linear function of the amount of fueling u_f and engine speed ω_e in an operating range. The range is defined as the set F of feasible controls and engine speeds,

$$F = \{u_f, \omega_e \mid 0 \leq u_f \leq u_{f,max}(\omega_e), \omega_{e,min} \leq \omega_e \leq \omega_{e,max}\} \tag{3.24}$$

where $\omega_{e,min}$ and $\omega_{e,max}$ are constants. The upper fueling bound is modeled as

$$u_{f,max}(\omega_e) = a_f\omega_e^2 + b_f\omega_e + c_f \tag{3.25}$$

where a_f, b_f, c_f are constants. In the operating range, the engine torque (3.1) is described by

$$T_e(\omega_e, u_f) = a_e\omega_e + b_e u_f + c_e \tag{3.26}$$

where a_e, b_e, c_e are constants. The fuel consumption is given by (3.23).

The prediction model will be transformed to be dependent on position rather than time. Denoting traveled distance with s and the trip time with t, then for a function $h(t(s))$

$$\frac{dh}{ds} = \frac{dh}{dt}\frac{dt}{ds} = \frac{1}{v}\frac{dh}{dt} \tag{3.27}$$

is obtained using the chain rule where $v > 0$ is assumed. By using (3.27), the models can be transformed as desired.

3.1.12 Evaluation Model

The powertrain dynamics are given by (3.20) with resisting forces according to (3.10) to (3.12). The engine torque T_e is assumed to be dependent on the amount of fueling u_f and engine speed ω_e, see Equation (3.1). In the evaluation model, this function is interpolated from steady state measurements performed in a test cell. The fuel consumption is given by (3.23).

The different components are implemented in a simulation environment as a number of separate entities, see further in Chapter 6.

3.2 Criterion

This section deals with the formulation of a control criterion. The verbally stated objective is to minimize the energy required for a given drive mission. The fundamental trade off with this objective is between fuel use and trip time. One approach is to a constrain the available time for the mission. Another way is to include a measure of the trip time or a measure of the violation of the constraint in the criterion function. The use of a look-ahead horizon, which means that the horizon in the original problem is divided into smaller parts, makes it difficult to set a well-founded constraint for the look-ahead horizon. Therefore, the trip time will be included in the criterion.

3.2.1 Continuous Formulation

The prediction model is expressed with traveled distance as the independent variable. Hence, to consider the trip time in the criterion either the time or velocity trajectory can be used. In the following, these two methods are used to devise control criteria. The first proposed function is based on the use of a velocity constraint and an inclusion of a measure of violation. The second proposal includes a direct measure of the trip time in the criterion.

The two proposed criteria will now be formulated mathematically. A step function denoted κ will be used in the following,

$$\kappa(e) = \begin{cases} 1, & e \geq 0 \\ 0, & e < 0 \end{cases} . \tag{3.28}$$

The fuel mass, denoted M, is a central quantity. On a trip from $s = s_0$ to $s = s_f$,

$$M = \int_{s_0}^{s_f} \frac{1}{v} \dot{m}(x, u) ds \tag{3.29}$$

where $\frac{1}{v}\dot{m}(x, u)$ is the mass flow per unit length as function of the states x and control u.

Velocity Penalty

Suppose there is a desired cruising speed denoted v_r. The criterion may then include a measure of the amount of disagreement between the velocity trajectory and v_r. However, only velocities above v_r should be penalized. Define the deviation e from the desired speed v_r as

$$e(v) = v_r - v \tag{3.30}$$

where v is the vehicle velocity. A measure of the violation P of the bound over a route is then

$$P = \int_{s_0}^{s_f} e^2 \kappa(e) ds \tag{3.31}$$

where κ is the step function (3.28) that only is non-zero when the bound is violated, that is when $v \leq v_r$. The trip time is thus taken into account implicitly by first stating a constraint on the velocity trajectory and then including a measure of the constraint violation into the criterion.

To weigh fuel and time use, the cost function is chosen as

$$I = M + \beta P \tag{3.32}$$

where β is a scalar factor that can be tuned to receive the desired trade off.

Time Penalty

The trip time T is simply

$$T = \int_{s_0}^{s_f} \frac{ds}{v}. \tag{3.33}$$

To weigh fuel and time use, the cost function chosen is

$$I = M + \beta T \tag{3.34}$$

where β is a scalar factor that can be tuned to receive the desired trade off.

3.2.2 Stationary Analysis

A stationary model is derived to facilitate analysis for the purpose of determining criterion parameters. The introduction of the look-ahead horizon raises the need to study how to choose the terminal cost. Under the assumption that there is a stationary solution, the model is used to show how the criterion parameters can be chosen in order to receive a desired trade off between fuel and time use.

Stationary Model

A model that assumes constant states $\hat{x}$ and controls $\hat{u}$ is now to be derived. The gear state and gear control signal are assumed to be identical to a given gear number. The brake control is assumed to be zero.

Assume that there exists at least one fueling level $\hat{u}_f$ for the given gear, for which the bounds in (3.25) holds and that gives a stationary velocity $\hat{v}$. From the prediction model in Section 3.1.11, the resisting forces (3.10)-(3.12), the driveline and engine equations (3.20) and (3.26), it is concluded that the control $\hat{u}_f$ can be written as

$$\hat{u}_f = c_1 \hat{v}^2 + c_2 \hat{v} + f(\alpha) \tag{3.35}$$

where

$$\begin{aligned} c_1 &= \frac{r_w c_w A_a \rho_a}{2 i \eta b_e}, \quad c_2 = -\frac{i}{r_w}\frac{a_e}{b_e} \\ f(\alpha) &= \frac{m g_0 r_w}{i \eta b_e}\left(c_r \cos\alpha + \sin\alpha\right) - \frac{c_e}{b_e} \end{aligned}$$

where c_1 and c_2 are constants and $f(\alpha)$ is a function corresponding to the rolling resistance and gravity, and thus being a function of the road slope α.

From Equation (3.22) and (3.27), it is concluded that the mass flow of fuel per unit length is directly proportional to the control $\hat{u}_f$ for the given gear,

$$\frac{1}{v}\dot{m}(x,u) = c_4 \hat{u}_f, \quad c_4 = \frac{n_{cyl}}{2\pi n_r}\frac{i}{r_w} \tag{3.36}$$

where c_4 is the proportionality constant.

Velocity Penalty

With the control $\hat{u}_f$ in (3.35), the cost function (3.32) is

$$\hat{I}(\hat{v}) = \begin{cases} \int_{s_0}^{s_f} \left(c_4 \left(c_1 \hat{v}^2 + c_2 \hat{v} + f(\alpha) \right) + \beta e(\hat{v})^2 \right) ds, & \hat{v} \leq v_r \\ \int_{s_0}^{s_f} \left(c_4 \left(c_1 \hat{v}^2 + c_2 \hat{v} + f(\alpha) \right) \right) ds, & \hat{v} > v_r \end{cases} \tag{3.37}$$

where the integrands clearly are constant with respect to s if a constant slope is assumed. A stationary point to $\hat{I}$ is found by setting the derivative equal to zero,

$$\frac{d\hat{I}}{d\hat{v}} = \int_{s_0}^{s_f} \left(c_4 \left(2c_1 \hat{v} + c_2 \right) - 2\beta e(\hat{v}) \right) ds = 0 \tag{3.38}$$

if $\hat{v} \leq v_r$. Solving the equation for β gives

$$\beta = \frac{c_4}{2e(\hat{v})} \left(2c_1 \hat{v} + c_2 \right) \tag{3.39}$$

and can be interpreted as the value of β such that a stationary velocity $\hat{v} \leq v_r$ is the solution to (3.38). Note that $e(\hat{v}) \to 0$, $\beta \to \infty$. This means that it is not possible to achieve a solution exactly v_r of the criterion with any finite β. With an optimization approach that quantizes the state space, the discrepancy e can be chosen to a value in the magnitude of the quantization level. If $\hat{v} > v_r$ the factor β has no influence on the cost function (3.32) and can therefore not be used to control the stationary solution.

Time Penalty

With the control $\hat{u}_f$ in (3.35), the cost function (3.34) is

$$\hat{I}(\hat{v}) = \int_{s_0}^{s_f} \left(c_4 \left(c_1 \hat{v}^2 + c_2 \hat{v} + f(\alpha) \right) + \frac{\beta}{\hat{v}} \right) ds \tag{3.40}$$

where the integrand clearly is constant with respect to s if a constant slope is assumed. A stationary point to $\hat{I}$ is found by setting the derivative equal to zero,

$$\frac{d\hat{I}}{d\hat{v}} = \int_{s_0}^{s_f} \left(c_4 \left(2c_1 \hat{v} + c_2 \right) - \frac{\beta}{\hat{v}^2} \right) ds = 0. \tag{3.41}$$

Solving the equation for β gives

$$\beta = c_4 \hat{v}^2 \left(2c_1 \hat{v} + c_2 \right) \tag{3.42}$$

and can be interpreted as the value of β such that a stationary velocity $\hat{v}$ is the solution to (3.41). Note that the value of β neither depends on the vehicle mass m nor the slope α. The calculated β will thus give the solution $\hat{v}$ of the criterion for any fixed mass and slope as long as there exists a control $\hat{u}_f$ satisfying the bounds in (3.25).

4

Dynamic Programming

The dynamic programming technique (DP) became a methodical instrument for optimization following the works of Bellman (Bellman, 1957, 1961; Bellman and Dreyfus, 1962). These works started to uniform the theory and showed the wide scope of applicability of DP. Research that further developed, explained and investigated aspects of the theory and demonstrated applications were initiated (Larson and Casti, 1978; Denardo, 1982; Bertsekas, 1995).

Dynamic programming for deterministic multi-stage decision processes will be studied in this chapter. The theory will be surveyed and discretization and computational aspects will be discussed.

4.1 Review of the Theory

The system studied is a deterministic multi-stage decision process described by

$$x_{k+1} = f_k(x_k, u_k), \quad k = 0, 1, \ldots, N-1 \tag{4.1}$$

where k denotes the stage number. The state vector x is n-dimensional and the control vector u is m-dimensional,

$$\begin{aligned} x_k &\in S_k \subset R^n \\ u_k &\in U_k(x) \subset R^m \end{aligned} \tag{4.2}$$

where it is clearly expressed that the admissible states S_k and controls $U_k(x)$ may vary with stage and state. The initial conditions

$$x(0) = x_0 \tag{4.3}$$

are given. A performance criterion is stated in the form

$$\zeta_N(x_N) + \sum_{i=0}^{N-1} \zeta_i(x_i, u_i) \tag{4.4}$$

where ζ_N is the terminal cost and ζ_i defines the intermediate costs. Denote the minimum value of the criterion $J_0^*(x_0)$, then

$$J_0^*(x_0) = \min_{u_0,\ldots,u_{N-1}} \zeta_N(x_N) + \sum_{i=0}^{N-1} \zeta_i(x_i, u_i) \tag{4.5}$$

is the problem faced.

The concept of DP is the *Principle of optimality*:

> An optimal policy has the property that whatever the initial state and initial decision are, the remaining decisions must constitute an optimal policy with regard to the state resulting from the first decision. (Bellman, 1957, p. 83)

The principle is easily justified by contradiction. Assume that an optimal policy P is found. At stage i, if the remaining truncated policy p is not optimal from stage i there is another policy p' from this stage with a lower cost. If p was replaced with p' in the entire policy P, the total cost for P would then be lowered which contradicts the fact that P is optimal.

The DP solution to the problem (4.5) is to solve the functional equation

$$J_k(x_k) = \min_{u_k} \{\zeta_k(x_k, u_k) + J_{k+1}(f_k(x_k, u_k))\} \tag{4.6}$$

for $k = N-1, N-2, \ldots, 0$ starting from

$$J_N(x_N) = \zeta_N(x_N) \tag{4.7}$$

being the terminal cost. When finished,

$$J_0^*(x_0) = J_0(x_0) \tag{4.8}$$

is the minimum cost. In a DP algorithm that proceeds backwards from the last stage, the entity $J_{k+1}(f_k(x_k, u_k))$ is called the cost-to-go since it is the minimum cost from a state $x_{k+1} = f_k(x_k, u_k)$ to an end state.

The recurrence equation (4.6) follows from the principle of optimality. Straightforward rewrites also show that the algorithm yields the desired minimum (Larson and Casti, 1978; Bertsekas, 1995). Analogous to Equation (4.5), denote with

$$J_k^*(x_k) = \min_{u_k,\ldots,u_{N-1}} \zeta_N(x_N) + \sum_{i=k}^{N-1} \zeta_i(x_i, u_i) \tag{4.9}$$

the minimum criterion value at stage k for a state x_k. This entity is rewritten to (4.6) by

$$\begin{aligned} J_k^*(x_k) &= \min_{u_k,\ldots,u_{N-1}} \left\{ \zeta_N(x_N) + \sum_{i=k}^{N-1} \zeta_i(x_i, u_i) \right\} \\ &= \min_{u_k} \min_{u_{k+1},\ldots,u_{N-1}} \left\{ \zeta_k(x_k, u_k) + \zeta_N(x_N) + \sum_{i=k+1}^{N-1} \zeta_i(x_i, u_i) \right\} \\ &= \min_{u_k} \left\{ \zeta_k(x_k, u_k) + \min_{u_{k+1},\ldots,u_{N-1}} \left\{ \zeta_N(x_N) + \sum_{i=k+1}^{N-1} \zeta_i(x_i, u_i) \right\} \right\} \\ &= \min_{u_k} \left\{ \zeta_k(x_k, u_k) + J_{k+1}(f_k(x_k, u_k)) \right\}. \end{aligned}$$

The first step uses the definition (4.9). The second step splits the minimization and the summation into two parts. In the third step, the minimization over $u_{k+1}, \ldots, u_{N-1}$ is moved inside the first set of brackets since it does not affect the term $\zeta_k(x_k, u_k)$. The last step is the identification of the term $J_{k+1}(f_k(x_k, u_k))$ where $x_{k+1} = f_k(x_k, u_k)$ from Equation (4.6). The minimum value $J_0^*(x_0)$ of the criterion (4.4) can thus be obtained by solving Equation (4.6) for $k = N-1, N-2, \ldots, 0$.

4.2 Discretization

In a straightforward DP approach, continuous state and control variables are discretized. The choice of grid granularity is a trade off between accuracy and complexity. A finer grid generally gives a better approximation to the original problem but an increased complexity.

For the purpose of an illustration, let x_k^i denote the quantized state i in stage k. Further, denote with $u_k^{i,j}$ the quantized control j that is applied in state i at stage k. A state x_{k+1} in the next stage is then given by $x_{k+1} = f(x_k^i, u_k^{i,j})$ and a cost $\zeta_k(x_k^i, u_k^{i,j})$ is incurred. The algorithm (4.6) can now be illustrated as shown in Figure 4.1. The minimum for every state of the transition cost for a control and the cost-to-go of the state resulting from the control is sought.

4.2.1 Interpolation

Interpolation may become necessary in a DP algorithm. The simplest methods to accomplish this are to use the nearest grid point or through linear interpolation of adjacent grid points. This issue was pointed out in e.g. Bellman and Dreyfus (1962) and these simple ways are still commonly used. The linear interpolation approach will be outlined in the following.

A need for interpolation can arise when evaluating the recurrence equation (4.6). When computing $x_{k+1} = f_k(x_k, u_k)$ at the state grid point x_k with

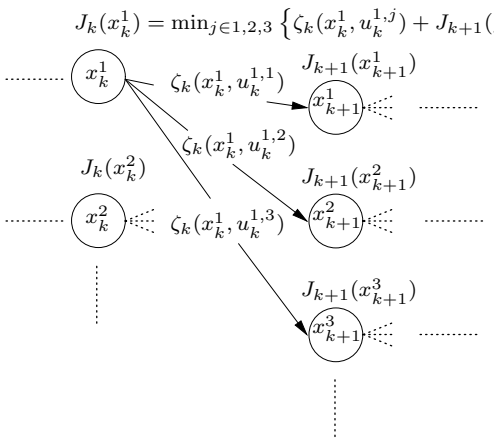

Figure 4.1: Illustration of the dynamic programming algorithm.

a discretized value of u_k, a state grid point will probably not be hit exactly, see the left part of Figure 4.2. The value of the cost-to-go $J_{k+1}(f_k(x_k, u_k))$ must then be approximated. One way is interpolation between the costs at adjacent states. For example, if a computed state x can be written as

$$x = \sum_{i=j}^{j+1} \xi^i x^i, \quad x^j \leq x \leq x^{j+1} \tag{4.10}$$

where x^i are the grid points, then

$$\hat{J}(x) = \sum_{i=j}^{j+1} \xi^i J(x^i). \tag{4.11}$$

is a linearly interpolated cost-to-go.

If the optimal trajectory is to be recovered when the DP algorithm is finished, another traversing of the stages is needed. When computing the system equation at a state grid point with the stored optimal control, another state grid point will probably not be hit exactly, see the right part of Figure 4.2. The resulting state and the optimal decision from that state must then be approximated. If the computed state can be written as in (4.10), a linear interpolation scheme set the interpolated control to

$$\hat{u} = \sum_{i=j}^{j+1} \xi^i u^i \tag{4.12}$$

where u^i is the optimal control from the state x^i.

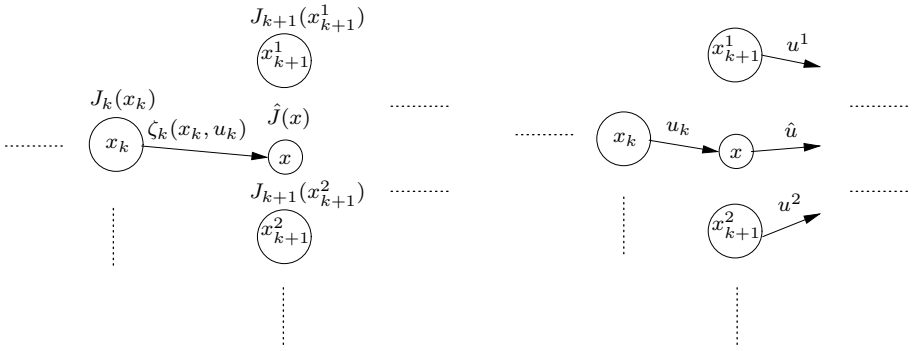

Figure 4.2: Left: Interpolating the cost-to-go $\hat{J}(x)$ when finding the optimal solution. Right: The optimal control $\hat{u}$ is interpolated when recovering the solution.

4.3 Computational Aspects

In the following, some aspects of a numerical solution with the DP algorithm will be examined. The different contributions to the computational complexity will be studied and techniques to reduce complexity and increase the accuracy are proposed.

4.3.1 Complexity

The computational complexity is determined by the dimensions and the number of quantization levels used for the state and control spaces. Denote with N_i the number of levels of state variable i and with M_i the number of levels of the control variable j. The total number of state grid points is then N_x and the total number of discrete controls N_u,

$$N_x = \prod_{i=1}^{n} N_i \quad N_u = \prod_{j=1}^{m} M_j, \tag{4.13}$$

where n, m are the dimensions of the state and control spaces respectively. With a horizon of N steps, the required computation time becomes

$$T = kNN_xN_u \tag{4.14}$$

where k is a constant. The constant is dependent on the specific implementation but mainly on the capacity and speed of the available computer hardware. From Equation (4.13) and (4.14) it is evident that the complexity grows exponentially with the dimensions of the state and control spaces.

The storage requirements are related to the dimension of the state space grid, N_x. If the minimum cost and the optimal decision are stored for each

state, the number of storage locations is

$$M = (m+1)NN_x. \tag{4.15}$$

For an illustration assume two state variables, two control variables and a horizon of twenty steps where each quantity is made discrete with one hundred quantization levels. The effort with dynamic programming is $T = k \cdot 20 \cdot 10^{4+4} = k \cdot 2 \cdot 10^9$ according to (4.14). For comparison, brute enumeration must consider the number of combinations of the control levels for the length of the horizon. This yields $T = k \cdot \left(10^4\right)^{20} = k \cdot 10^{80}$ as an approximation of the computation time. If each calculation requires about ten floating point operations and the hardware could do 10^9 operations per second[1], the constant k becomes in the order of 10^{-8}. DP would then finish in about 20 seconds but the enumeration procedure would require substantially more time. The number of memory locations becomes $M = 6 \cdot 10^5$. Using a single-precision floating point representation with 32 bits renders a memory requirement of about 2.3 megabytes[2].

4.3.2 State Space

The number of state grid points N_x adds to the complexity multiplicatively according to (4.14). If the grid size is kept but the volume of the state space that is searched can be reduced a priori without loosing solutions to the original problem, the complexity is reduced.

The volume of the state space that is searched for the solution is called the search space and is made up of the feasible states given in (4.2). The system model (4.1) can further be used to reduce the search space by removing unreachable and undesired states. The unreachable states are the states that are not possible to attain with all the admissible controls for the system model. A trajectory through an undesired state will inevitable violate the feasible bound at some later time.

The problem to find the reachable states can be formulated as an optimization problem with the objective to maximize the rate by which the state vector changes. The undesirable states are not in general determined in a straightforward way. However, in a specific application there may be ways to analytically or approximately identify some states as undesired. In (Back, 2006), similar concepts to infeasible and unreachable sets are used for a first-order system and optimal control theory is utilized to find these sets.

4.3.3 Control Space

Quantization of the control space gives rise to the need for interpolation as explained earlier. If the system equations are possible to invert, it can be used

[1] One GFLOPS is equivalent to 10^9 floating point operations per second which most standard personal computers of today slightly exceeds.

[2] In order to reach the limit for fast memory of a current standard personal computer, the value of M must approach about 10^8.

to avoid interpolation. Rather than testing quantized values, the control for a state transition is calculated. Since no grid size has to be selected for the control, the number of algorithm parameters is reduced. However, inversion of the system equations may be difficult, time consuming or even impossible.

If the method is possible to apply, the number of controls N_u that have to be evaluated for each state is limited by the number of state grid points N_x. The required computation time would hence increase with the square of the number of state grid points N_x,

$$T = kNN_x^2 \tag{4.16}$$

according to (4.14) where k is a constant and the horizon has N steps.

Optimality Guided Fast Search

For a first-order system, the method of calculating rather than quantizing the control can be combined with a search method better than the straightforward one. The idea relies on the observation that, provided that the discretization grid used is sufficiently fine-grained, optimal paths can not cross each other due to the principle of optimality. The set of states that is to be traversed is sorted in order and then divided into two parts repeatedly. The optimal controls already calculated will then limit the set of states that is needed to be processed.

Figure 4.3 depicts an example. The search space is shaded in gray. The states are dots and optimal controls are shown with arrows. The set of states that is reachable from one stage to the next is indicated with dashed lines. The states are assumed to be sorted in order from the lower to the upper bound. To the left a state near the middle is selected in a stage k. The optimal decision is then searched for by calculating the required control, if it exists, to the reachable states in the next stage $k+1$. For this instant, the reachable set of states was a subset of the states in the next stage. The next step is to select two states near the middle of the respective parts in stage k. The optimal control from the previous iteration will now limit the set of states that needs to be searched. For this iteration, there are reachable states outside the search space but since it is assumed that optimal paths do not cross, there is no need to consider these. The procedure is then continued until all states have been processed.

Let $N_x = 2^n$ denote the number of states per stage. In the first iteration one state is selected in the current stage k and at maximum N_x states is considered in the next stage $k+1$. The next iteration selects two states in the stage k and the maximum number of states to consider in stage $k+1$ is still N_x. The states in stage k can be divided by two n times. The total number of combinations that has to be considered is then

$$\sum_{i=1}^{n} N_x = nN_x = n2^n = N_x \log_2 N_x$$

where $\log_2$ denotes the logarithm with base 2. The required time can now be estimated by

$$T = kNN_x \log_2 N_x \tag{4.17}$$

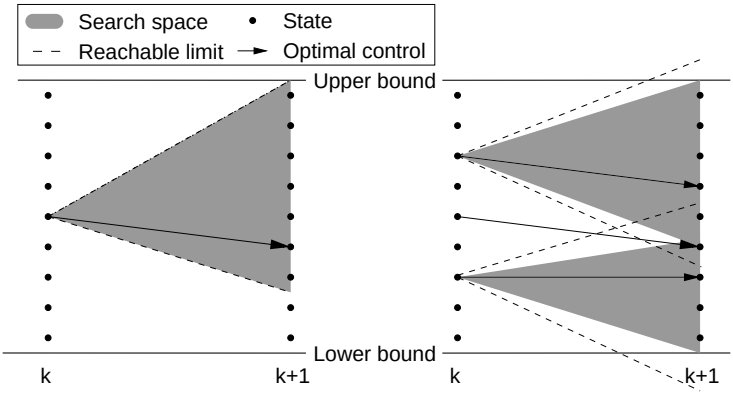

Figure 4.3: Two iterations of a DP search method. Left: The reachable states and the constraints limit the search space at first. Right: In subsequent iterations the search space is also limited by previously calculated optimal controls.

which should be compared with (4.16). The complexity dependency on the number of state grid points N_x is thus reduced from N_x^2 to $N_x \log_2 N_x$.

5

A Fuel-optimal Algorithm

The look-ahead control strategy is a predictive control scheme where the problem in each iteration is truncated, discretized and solved by dynamic programming algorithm. This chapter formulates the optimization algorithm. The aim is a fuel-optimal algorithm by which it is possible to obtain satisfactory solutions in real-time on-board a vehicle. An analysis will be undertaken to investigate numerical properties of the algorithm that are shown to be crucial for satisfactory performance.

5.1 Constraints

The allowed velocities are, according to the problem formulation in Section 2.1, constrained to a set that is determined by e.g. acceptable trip time in combination with legal and safety considerations. Let s be the position along the route, i.e. the traveled distance. Denote the vehicle velocity v, then

$$A = \{v \mid v_{min}(s) \leq v \leq v_{max}(s)\} \tag{5.1}$$

is the allowed interval. In this chapter, the bounds will be considered constant over the horizon. The brake system is assumed to be powerful enough to keep the upper bound v_{max}. On the other hand, the lower bound v_{min} is not expected to be feasible over the entire horizon on all road profiles. Though, it is assumed that it is possible to keep a velocity, denoted $v_{lim}(s)$, which is positive at all times. If Equation (5.1) was to be used, it would not be certain to find any feasible solution. Therefore, the constraints on the vehicle speed v are expressed

as,

$$A = \{v \mid \min\{v_{min}, v_{lim}(s)\} \leq v \leq v_{max}\}. \tag{5.2}$$

5.2 Discrete Prediction Model

Since the approach in this chapter is numerical, the prediction model and the look-ahead horizon should be made discrete. The prediction model given in Chapter 3 is used, having the velocity and the engaged gear making up the state vector, the fueling, brake level and gear selector as control signals and the road slope as a measurable disturbance. The horizon will be divided into equidistant steps denoted h.

The value of the state vector $x(s)$ at stage k will be denoted

$$x_k = \begin{bmatrix} v_k \\ g_k \end{bmatrix} = x(kh) \tag{5.3}$$

where v_k, g_k is the velocity and engaged gear. The control signals $u(s)$ will be considered piece-wise constant during a step,

$$u_k = \begin{bmatrix} u_f \\ u_b \\ u_g \end{bmatrix} = u(kh) \tag{5.4}$$

where u_f controls the fueling, u_b determines the braking torque and u_g selects gear. Finally, the road slope α_k is set to the mean value over the step,

$$\alpha_k = \frac{1}{h}\int_{kh}^{(k+1)h} \alpha(s)ds. \tag{5.5}$$

The system dynamics is thus

$$x_{k+1} = f(x_k, u_k, \alpha_k) \tag{5.6}$$

where $f(x_k, u_k, \alpha_k)$ is given by (3.20) and (3.9). The output is the integral of the fuel flow (3.22).

5.3 Discrete Criterion

The continuous criteria was formulated in Chapter 3. The approach in this chapter is numerical and the criterion should therefore be made discrete. With the notation from Chapter 3, denote

$$\begin{aligned} m_k &= \int_{kh}^{(k+1)h} \frac{1}{v}\dot{m}(x,u)ds, \quad t_k = \int_{kh}^{(k+1)h} \frac{ds}{v}, \\ p_k &= \int_{kh}^{(k+1)h} e^2\kappa(e)ds. \end{aligned} \tag{5.7}$$

A quantization of the state and control spaces may lead to that the solution switches frequently between neighboring grid points. In order to enable smoothing of the numerical solution the terms

$$a_k = |v_k - v_{k+1}| \quad b_k = \kappa(|g_k - g_{k+1}|) \tag{5.8}$$

are introduced where κ is the step function (3.28).

The discrete cost function is expressed as

$$J = \zeta_N + \sum_{k=0}^{N-1} \zeta_k(x_k, x_{k+1}, u_k, \alpha_k) \tag{5.9}$$

where ζ_k is the running cost and ζ_N the terminal cost.

5.3.1 Running Cost

For the criterion (3.32) with the velocity penalty, the weighting function ζ_k for stage k is chosen as

$$\zeta_k = [1, \beta, \gamma, \vartheta] \begin{bmatrix} m_k \\ p_k \\ a_k \\ b_k \end{bmatrix}, \quad k = 0, 1, \ldots, N-1 \tag{5.10}$$

where β, γ, ϑ are scalar penalty parameters for controlling the properties of solutions.

The weighting functions for the criterion (3.34) with the penalty on the trip time become

$$\zeta_k = [1, \beta, \gamma, \vartheta] \begin{bmatrix} m_k \\ t_k \\ a_k \\ b_k \end{bmatrix}, \quad k = 0, 1, \ldots, N-1 \tag{5.11}$$

where β, γ, ϑ are, again, scalar penalty parameters for controlling the properties of solutions.

5.3.2 Terminal Cost

As described in Chapter 2, the DP formulation is an approximation of the problem where the horizon is truncated to N steps. The approach is to choose an approximation of the cost-to-go for the problem over the entire horizon. Known methods for approximation involve offline and online calculations. One offline approach is to simplify the present model and use it for deriving the approximation. Online calculations can e.g. be based on a heuristic control law where the cost is computed analytically or through simulations. (Bertsekas, 1995, 2005)

In the present work the terminal cost is set to zero and instead, the terminal states are constrained. This will be exploited in a preprocessing stage to further reduce the search space prior to the application of the DP algorithm. A well chosen terminal cost can probably approximate the solution to the original problem in a better way, although it may come at the cost of a slightly increased complexity. However, the better the terminal cost approximation the shorter look-ahead horizon is needed which also would reduce complexity.

5.4 Preprocessing

As mentioned in Chapter 4, the number of state grid points N_x that are used in the DP algorithm will add to the complexity multiplicatively. If, for a fixed quantization, the volume of the state space that is searched can be reduced a priori the complexity may be reduced.

The search space X^{SS}, is a subset of the entire state space X. The set A of allowed velocities is defined by the problem formulation, see Equation (5.2). To determine A and the set of reachable states, denoted R, the prediction model is simulated. Maximum and minimum torque is assumed to be obtained with maximum and minimum fueling respectively. All feasible gears are tried to find the gear giving maximum acceleration with maximum torque.

The terminal states are constrained and assigned a terminal cost of zero as explained. This is done after the reachable set has been determined by a forward simulation. The horizon is then traversed backwards in order to remove the states U that are undesired.

Finally, the states belonging to A and R but not U determines the search space,

$$X^{SS} = (A \cap R) \setminus U. \tag{5.12}$$

One example is given in Figure 5.1 where the respective sets are indicated. The allowed set A is given by the problem formulation. With a set of initial and terminal states specified, the reachable states R and the undesired states U are determined by the maximum acceleration and deceleration.

5.5 A DP Algorithm

To summarize, the optimal control problem at hand is the minimization of the objective,

$$\min_u \sum_{k=0}^{N-1} \zeta_k(x_k, x_{k+1}, u_k, \alpha_k)$$

where ζ_k is given by the selected objective in Section 5.3. The system dynamics is given by

$$x_{k+1} = f(x_k, u_k, \alpha_k) \quad k = 0, 1, \ldots, N-1$$

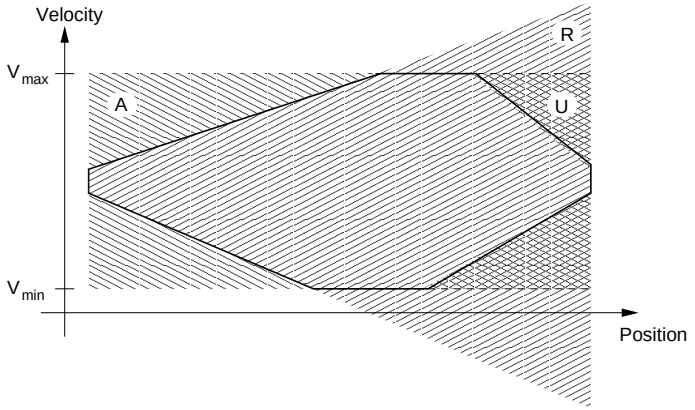

Figure 5.1: Search space example.

according to (5.6). The constraints are

$$0 < \min\{v_{min}, v_{lim}(kh)\} \leq v_k \leq v_{max} \quad k = 0, 1, \ldots, N-1$$

according to (5.2). Due to the rolling horizon setting, the initial state x_0 is given.

The preprocessing algorithm gives, for each stage, an interval of velocities that are to be considered. For every stage the interval $[v_{lo}, v_{up}]$ is discretized in constant steps of δ. This makes up a set V_k,

$$V_k = \{v_{lo}, v_{lo} + \delta, v_{lo} + 2\delta, \ldots, v_{up}\}. \tag{5.13}$$

With a given velocity, only a subset of the gears in the gearbox is feasible. If the operating region of the engine is defined with bounds on the engine speed $[\omega_{e,min}, \omega_{e,max}]$, it is easy to select the set of feasible gears. Only gears with a ratio that gives an engine speed in the allowed range are then considered. In a state with the velocity v, the set of usable gears G_v is thus defined as

$$G_v = \{g \mid \omega_{e,min} \leq \omega_e(v, g) \leq \omega_{e,max}\} \tag{5.14}$$

where $\omega_e(v, g)$ is the engine speed at vehicle velocity v and gear number g.

Braking is only considered in the algorithm if the upper velocity bound is encountered. Braking without recuperation is an inherent waste of energy and therefore braking will only occur when the velocity bounds would otherwise be violated. This reduces the complexity since the number of possible control actions lessens.

A state x is made up of velocity v and gear number g. The possible states in stage k are denoted with the set S_k and it is generated from the velocity range V_k given in (5.13) and the set of gears G_v given in (5.14). This yields

$$S_k = \{\{v, g\} \mid v \in V_k,\ g \in G_v\}. \tag{5.15}$$

Standard Approach

For the standard approach the controls needs to be discrete. The fueling u_f and braking u_b are normalized and then quantized in constant steps. Possible values of the gear control u_g are given by the finite and discrete set of usable gears (5.14).

For each state x_k in stage k, all combinations of fueling levels and gears are applied to the system. The next state x_{k+1} and the cost ζ_k is given by evaluating the system equations. The cost-to-go $J_{k+1}(x_{k+1})$ is linearly interpolated from the neighboring grid points as described in Section 4.2.1. If the simulated state x_{k+1} is written as

$$x_{k+1} = \sum_{i=j}^{j+1} \xi^i x^i, \qquad \begin{matrix} v^j \leq v \leq v^{j+1} \\ g^j = g = g^{j+1} \end{matrix} \tag{5.16}$$

where x^i are the grid points in stage $k+1$, then

$$\hat{J}_{k+1}(x_{k+1}) = \sum_{i=j}^{j+1} \xi^i J(x^i). \tag{5.17}$$

is the interpolated cost-to-go.

If no feasible control is found from the state x^i, all quantized braking levels are applied to the system. If still no feasible controls are found, the cost-to-go $J_k(x^i)$ is set to infinity, which with a numerical approach means a very large number.

The algorithm is outlined below. The set U_k denotes the set of allowed controls, that is all combinations of either fueling levels u_f or braking levels u_b and the gear control u_g.

1. Let $J_N(x) = 0$.
2. Let $k = N - 1$.
3. Let
$$J_k(x) = \min_{u \in U_k} \left\{ \zeta_k(x, u) + J_{k+1}(f(x, u)) \right\}, \quad x \in S_k.$$
4. Repeat (3) for $k = N-2, N-3, \ldots, 0$.
5. The optimal cost is J_0, and the sought control is the set of optimal controls from the initial state.

If the optimal solution for the entire horizon is to be recovered, the optimal controls probably needs to be interpolated as explained in Section 4.2.1. If the state is written as in (5.16), the interpolated control $\hat{u}$ become

$$\hat{u} = \sum_{i=j}^{j+1} \xi^i u^i \tag{5.18}$$

where u^i is the optimal control from the state x^i.

Inverse Approach

The inverse approach is an alternative to the standard approach where the control for a state transition is calculated instead of testing quantized levels. At a stage k, feasible control actions $u_k^{i,j}$ that transform the system from a state $x^i \in S_k$ to another state $x^j \in S_{k+1}$ are sought. The control is found by an inverse simulation of the system equations. If there are no fueling level u_f and gear u_g that transforms the system from state x^i to x^j at stage k, there are two possible resolutions. If there exist a feasible braking control u_b the cost of the transition is set accordingly. If there is no feasible braking control the cost is set to infinity.

When the gear state is neutral gear $g = 0$ inverse simulation is not possible and a forward simulation is performed. The cost-to-go is then taken as the nearest grid point.

The algorithm is outlined below.

1. Let $J_N(i) = 0$.
2. Let $k = N - 1$.
3. Let
$$J_k(x^i) = \min_{x^j \in S_{k+1}} \left\{ \zeta_k^{i,j} + J_{k+1}(x^j) \right\}, \quad x^i \in S_k.$$
4. Repeat (3) for $k = N - 2, N - 3, \ldots, 0$.
5. The optimal cost is J_0 and the sought control is the optimal control set from the initial state.

In this approach, the quantization of the controls is determined implicitly by the resolution of the state space grid and the number of algorithm parameters is thus reduced in comparison with the standard approach.

5.5.1 Summing up

Two criteria were proposed in Equation (3.32) and (3.34) with discrete formulations in Equation (5.10) and (5.11). The criterion for the present work is chosen as the latter since it besides the fuel mass includes a direct measure of the trip time and the basic trade off for fuel-optimal control is between these quantities. Results with the other criterion are given in Hellström et al. (2006).

The approach taken in the current work is the inverse approach, i.e. the method of inversely calculating the required control for a state transition. A benefit of this method is that there is no need to discretize the control and no interpolation of cost or control is therefore needed. It relies on that the model equations can be inverted which is true for a fixed gear. For the present problem, this methodology can further be combined with the fast search method explained in Section 4.3.3 in order to reduce complexity.

5.6 Numerical Analysis

Performing numerical optimization of dynamical systems inevitable leads to errors such as rounding and truncation errors. Floating point arithmetics always introduces a rounding error. If the original problem has continuous components, they must be given discrete approximations. This will, in general, give rise to truncation errors. It is of course desirable, but hard to guarantee, that such errors do not lead to that the numerical solution differ from the true solution to the original problem.

During the algorithm development solutions were obtained that were undesired. To avoid such behavior in the final algorithm both parameter tuning and analysis of guiding examples were performed. In the following first some potential problems that can occur are presented. These must be avoided, and therefore test problems and guiding examples are analyzed to accomplish this.

5.6.1 Potential Numerical Problems

Potential problems caused by numerical errors are presented in the following. The shown solutions are obtained by applying the inverse approach with the selected criterion (5.11). The prediction model in Section 3.1.11 are used and flat road is assumed. The grid is 20 steps of 50 m and a velocity quantization of 0.2 km/h is used.

Oscillating solutions are obtained when the Euler forward method is used to discretize the model equations. The forward method applied to the prediction model is stable for the step lengths used so a stability analysis can not explain the behavior. Figure 5.2 shows characteristic appearance. The oscillating solution obtained when using Euler forward is shown to the left. The more stable solution to the right is obtained with Euler backward. This type of behavior

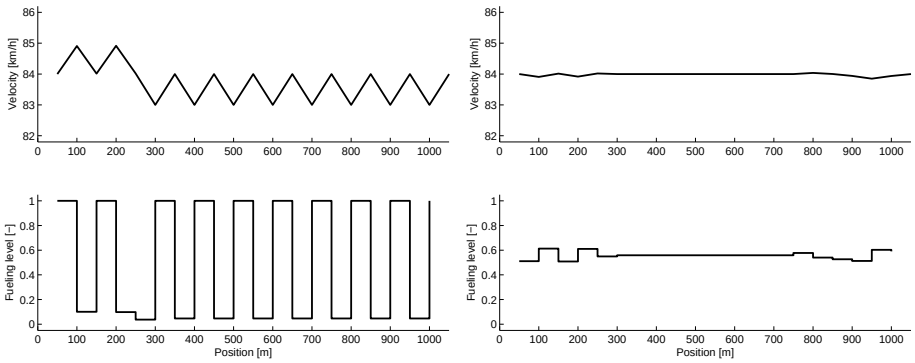

Figure 5.2: Using different methods to discretize the model used for optimization. Left: Euler forward. Right: Euler backward.

was seen both with the standard and the inverse approach. Using a finer grid

does not remove the behavior completely, but a very short step length or a lot of smoothing reduces the oscillations. However, a short step length gives more stages for the same horizon length in the DP algorithm and thus a higher complexity.

Allowing neutral gear gives irrational solutions with the inverse approach. An example of such a solution is seen to the left in Figure 5.3. When neutral gear is engaged, inverse simulation is not possible and, in general, the cost-to-go must be approximated. In the inverse approach, this is done by nearest neighbor interpolation. A bound on the overestimation of the state is derived in this section that is used to prevent the irrational solutions. When using this bound, the solution to the right in Figure 5.3 is obtained instead.

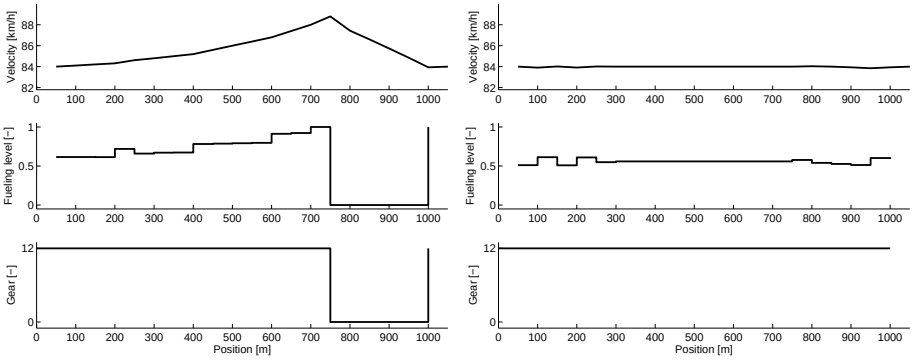

Figure 5.3: Left: Using nearest grid point interpolation. Right: Utilizing bound on state overestimation.

5.6.2 Test Problem

The test problem is the vehicle in Figure 2.1 (p. 8) with one additional assumption. The resisting force is assumed to be independent of x, that is $f(x, v) = f(v)$. The function is still assumed to be monotonically increasing for $v > 0$ according to Equation (2.1). A model for the system is given by (2.4),

$$mv\frac{dv}{dx} = g(u) - f(v). \tag{5.19}$$

The objective considered is to minimize the work needed to bring the system from $x = 0,\ v(0) = v_0$ to $x = s,\ v(s) = v_0$. According to (2.5), the work needed is

$$W = \int_0^s g(u)\ dx = \int_0^s f(v)\ dx \tag{5.20}$$

since the kinetic energy at the start and the end of the interval is the same. The time is constrained by

$$\int_0^s \frac{dx}{v} \leq T \tag{5.21}$$

Assume now that the entire horizon, i.e. the integration interval is subdivided into only three mesh points

$$0 < h < 2h \tag{5.22}$$

where h denotes the step size that equals half the horizon length. The control u is assumed constant on each subinterval,

$$u(x) = \begin{cases} u_0 & , \quad 0 \leq x < h \\ u_1 & , \quad h \leq x < 2h \end{cases}$$

The objective can then be stated as

$$J = \min_{u_0, u_1} h\left(g(u_0) + g(u_1)\right) \tag{5.23}$$

or equivalently

$$J = \min_{v_0, v_1} h\left(f(v_0) + f(v_1)\right) \tag{5.24}$$

using Equation (5.20) and where $v(0) = v_0$, $v(h) = v_1$. The maximum time T is chosen as

$$T = \frac{2h}{v_0}. \tag{5.25}$$

Using Equation (5.23) for interpretation, the problem is to choose the control u_0 and u_1 which gives v_1 as the intermediate velocity and v_0 as the end velocity such that the objective is minimized. By (5.24) the problem is interpreted as the selection of the intermediate velocity v_1, which implicitly determines the control, as to minimize the objective. The objective (5.24) will increase if $v_1 > v_0$. Since $v_1 < v_0$ would violate the time constraint (5.25), the optimal path is constant speed, $v_1 = v_0$.

5.6.3 Discretization Errors

The choice of discretization method affects algorithm complexity, and three well known and simple methods for solving ordinary differential equations are the Euler forward and backward method and the trapezoidal rule. The effects of using these methods on the test problem will be studied in the following.

The forward Euler method applied on the model (5.19) gives

$$\frac{v_{i+1} - v_i}{h} = \frac{dv}{dx}(x_i) = \frac{1}{mv_i}\left(g(u_i) - f(v_i)\right) \tag{5.26}$$

and Euler backward

$$\frac{v_{i+1} - v_i}{h} = \frac{dv}{dx}(x_{i+1}) = \frac{1}{mv_{i+1}}\left(g(u_i) - f(v_{i+1})\right) \tag{5.27}$$

and finally, the trapezoidal rule yields

$$\begin{aligned}\frac{v_{i+1}-v_i}{h} &= \frac{1}{2}\left(\frac{dv}{dx}(x_i)+\frac{dv}{dx}(x_{i+1})\right)\\ &= \frac{1}{2m}\left(\frac{g(u_i)-f(v_i)}{v_i}+\frac{g(u_i)-f(v_{i+1})}{v_{i+1}}\right).\end{aligned} \tag{5.28}$$

Now, study the value of the objective (5.23) when using these different methods. Letting $i = \{0, 1\}$, the equations (5.26) to (5.28) can be solved for $g(u_0)$ and $g(u_1)$ in each case. Due to the terminal constraints, $v_2 = v_0$. Insertion into the objective (5.23) gives when using the forward Euler method,

$$W_{EF}(v_0, v_1) = h\left(f(v_0) + f(v_1)\right) - m\left(v_1 - v_0\right)^2 \tag{5.29}$$

and when using the backward Euler method,

$$W_{EB}(v_0, v_1) = h\left(f(v_0) + f(v_1)\right) + m\left(v_1 - v_0\right)^2. \tag{5.30}$$

Using the trapezoidal rule yields

$$W_{TR}(v_0, v_1) = 2h\frac{v_0 f(v_1) + v_1 f(v_0)}{v_0 + v_1}. \tag{5.31}$$

In the following some observations are made from these basic calculations. Note that $f(v_1) > f(v_0)$ for $v_1 > v_0$ holds by the assumption (2.1).

Observations

Looking at the objective value (5.29) that is obtained when using the Euler forward method, it is seen that the expression might have a lower value for $v_1 > v_0$ than for $v_1 = v_0$. When using the Euler backward method (5.30) or the trapezoidal rule (5.31) it is seen that there is no $v_1 > v_0$ such that the objective becomes lower than when $v_1 = v_0$. The minimum of the objective is expected to occur for $v_1 = v_0$. Therefore, using the Euler forward method does not guarantee that the solution to the test problem is preserved. When using the Euler backward method and the trapezoidal rule, the solution to the test problem is still constant speed.

Studying only the first term of the Euler forward approximation (5.26), it is seen that the contribution to the motion from a given control u_i will always be overestimated if $v_{i+1} > v_i$. The opposite is true for the Euler backward approximation (5.27). The symmetric trapezoidal rule (5.28) include the mean of the overestimating and underestimating terms respectively. The problem is to find the control that minimizes a criterion that includes a measure of the required energy. Therefore, underestimating the required energy for certain control and state trajectories is unsound.

All three tried methods are known to be convergent and stable for sufficiently small step lengths but these concepts do not reveal if the known solution is

preserved for the test problem. Also note that if the same dynamical model (5.19) is used with an objective of maximizing instead of minimizing the criterion (5.20), the trapezoidal rule would not cause trouble but the Euler forward would instead be preferred over the Euler backward method for this test problem.

Alternative Problem Description

For the test problem, an alternative problem description can be achieved by using that

$$\frac{dv}{dt} = v\frac{dv}{dx} = \frac{1}{2}\frac{d}{dx}v^2$$

which yields

$$\frac{m}{2}\frac{d}{dx}v^2 = g(u) - f(v)$$

by using the governing dynamics in (5.19). By introducing the state y

$$y = \frac{1}{2}mv^2, \quad v = \sqrt{\frac{2}{m}y}$$

of kinetic energy instead of the velocity v,

$$\frac{dy}{dx} = g(u) - f(\sqrt{\frac{2}{m}y})$$

is obtained. The objective value (5.23) then becomes

$$W_{EF} = W_{EB} = W_{TR} = h\left(f(v_0) + f(v_1)\right)$$

regardless of which one of these methods that is used.

5.6.4 State Errors

To study state errors, two solution trajectories to the test problem are compared, see Figure 5.4. The first is the known optimal path with constant speed $v(x), x \in \{0, h, 2h\}$. The other is an oscillating trajectory with an intermediate speed $v(h) = v_1 > v_0$. The amount of perturbation in the intermediate velocity v_1 that gives the oscillating trajectory a lower objective value than the constant speed trajectory will be quantified.

In order to obtain explicit results, it will for this analysis be assumed that the resisting force is given by

$$f(v) = Cv^2 + D \tag{5.32}$$

where C, D are positive constants. The objective for the test problem is then

$$W = \int_0^s f(v)\, dx = C\int_0^s v(x)^2\, dx + Ds \tag{5.33}$$

according to (5.20).

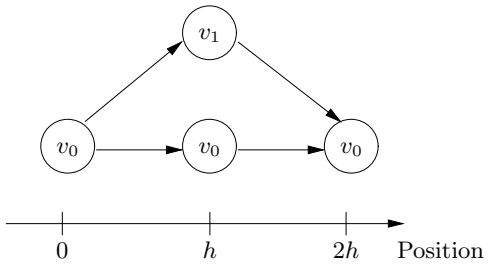

Figure 5.4: Two possible state trajectories for the test problem.

Exact Solution

The two paths in Figure 5.4 are studied. Denote the constant velocity function by v_c and a piece-wise continuous velocity function for the oscillating trajectory by v_a. Assume, for the oscillating trajectory, that the acceleration is constant and equals a,

$$\frac{dv_a}{dt} = \begin{cases} a, & 0 \leq x \leq h \\ -a, & h \leq x \leq 2h \end{cases} \tag{5.34}$$

where $a > 0$. Rewrite according to

$$\frac{dv}{dt} = \frac{dv}{dx}\frac{dx}{dt} = v\frac{dv}{dx} \tag{5.35}$$

then, integration yields

$$v(x) = \sqrt{2ax + 2c_0} \tag{5.36}$$

where c_0 is a constant determined by the initial condition, $v(0) = \sqrt{2c_0}$. The velocity functions can thus be written as

$$v_c(x) = v_0, \quad 0 \geq x \geq 2h \tag{5.37}$$

and

$$v_a(x) = \begin{cases} \sqrt{2ax + v_0^2}, & 0 \geq x \geq h \\ \sqrt{-2a(x-h) + v_1^2}, & h \geq x \geq 2h \end{cases} \tag{5.38}$$

using (5.36). Denote with W_o the objective value of the oscillating trajectory and with W_c the objective value of the constant speed trajectory. The difference ΔW_p is then

$$\Delta W_p = W_o - W_p = C\int_0^{2h} v_a(x)^2 - v_c(x)^2\, dx = Ch(v_1^2 - v_0^2) \tag{5.39}$$

according to Equation (5.33). This is the true difference in the work needed for the two paths.

Perturbed Solution

Introduce an error ϵ in the velocity v_1. The error can be interpreted as a gain or loss of kinetic energy, ΔW_k where

$$\Delta W_k = \frac{m}{2}((v_1+\epsilon)^2 - v_1^2) = \frac{m}{2}(\epsilon^2 + 2v_1\epsilon). \tag{5.40}$$

The solution can only be altered if the kinetic energy is overestimated, that is $\epsilon > 0$ is assumed from now on. If the error ΔW_k is greater than the unperturbed difference of the objective values ΔW_p, the oscillating trajectory becomes optimal. Therefore, define the function $e(\epsilon)$ as

$$\begin{aligned} e(\epsilon) &= \Delta W_p - \Delta W_k = Ch(v_1^2 - v_0^2) - \frac{m}{2}(\epsilon^2 + 2v_1\epsilon) \\ &= -\frac{m}{2}\epsilon^2 - 2v_1\epsilon + Ch(v_1^2 - v_0^2). \end{aligned} \tag{5.41}$$

using (5.39) and (5.40). If $e(\epsilon) > 0, \epsilon > 0$ holds, the solution is not altered. The roots of (5.41) are

$$\epsilon = -v_1 \pm \sqrt{v_1^2 + \frac{2Ch(v_1^2 - v_0^2)}{m}}$$

This yields two real roots r_1 and r_2 since it was assumed that $v_1 > v_0$. The second derivative of (5.41) is negative and $e(0) > 0$ and hence $e(\epsilon) > 0$ for $0 < \epsilon < r_2$ where r_2 is the larger root,

$$\begin{aligned} r_2 &= -v_1 + \sqrt{v_1^2 + \frac{2Ch(v_1^2 - v_0^2)}{m}} \\ &= v_1\left(-1 + \sqrt{1 + \frac{2Ch}{m}\left(1 - \left(\frac{v_0}{v_1}\right)^2\right)}\right). \end{aligned} \tag{5.42}$$

Since $\frac{2Ch}{m} > 0$,

$$r_2 > v_1\left(-1 + \sqrt{1}\right) = 0$$

holds, it is concluded that r_2 is positive, that is, there is a margin of error that can be accepted without altering the solution. Using a series expansion, (5.42) can be written as

$$\begin{aligned} r_2 &= v_1\left(-1 + 1 + \frac{1}{2}\left(\frac{2Ch}{m}\left(1 - \left(\frac{v_0}{v_1}\right)^2\right)\right) - \dots\right) \\ &\approx v_1\left(\frac{Ch}{m}\left(1 - \left(\frac{v_0}{v_1}\right)^2\right)\right) \\ &= v_1\left(\frac{Ch}{m}\left(1 + \frac{v_0}{v_1}\right)\left(1 - \frac{v_0}{v_1}\right)\right) \end{aligned} \tag{5.43}$$

and since $\frac{v_0}{v_1} \approx 1$, then $1 + \frac{v_0}{v_1} \approx 2$ which yields

$$r_2 \approx \frac{2Ch}{m}(v_1 - v_0) \geq 2h\delta\frac{C}{m} \tag{5.44}$$

where δ is the state quantization step. If the perturbation is less than this bound, the solution to the test problem is preserved. An oscillating solution with an amplitude of $\delta = v_1 - v_0$ can be insignificant with a fine grid. If an acceptable level of perturbation of the solution is denoted τ,

$$\tau = v_1 - v_0 = n\delta,\ n > 1$$

then

$$\epsilon < 2hn\delta\frac{C}{m} \tag{5.45}$$

should hold. Equation (5.45) shows how the physical parameters C, m and the optimization parameters h, δ influences the bound.

Numerical Values

Let the constant C in the resisting force model (5.32) correspond to the air drag, i.e.

$$C = \frac{1}{2}c_w\rho_a A_a$$

according to (3.10) where c_w is the air drag coefficient, A_a is a cross section area and ρ_a is the air density. For typical values of a truck,

$$C \approx \frac{1}{2} \cdot 0.6 \cdot 1.2 \cdot 10 = 3.6 > 3.$$

Studying heavy trucks, the mass m will be some ten tonnes but usually less than 60 tonnes. The optimization parameters should then satisfy (5.45) where

$$2hn\delta\frac{C}{m} > 2hn\delta\frac{3}{60 \cdot 10^3} = \frac{1}{2}10^{-4} \cdot 2hn\delta. \tag{5.46}$$

With a horizon length $2h$ of more than 1000 m, the bound (5.46) becomes $\frac{n}{2}10^{-1}\delta$. The allowed perturbation is thus about an order of a magnitude less than the quantization step δ.

When performing numerical computations on a computer, the floating point representation always gives a rounding error. The IEEE floating point standard (IEEE Standards Board, 1985) for single precision gives a relative rounding error less than

$$\frac{1}{2}2^{-23} < 5.97 \cdot 10^{-8}.$$

For a velocity about 90 km/h, that is 25 m/s, the absolute error becomes about $1.49 \cdot 10^{-6}$. Comparing this to Equation (5.46) with $n = 1$, it is seen that if

$$2h\delta > 0.03$$

holds, the margin will be greater than the floating point accuracy. Thus, the used precision sets a bound on how fine a usable grid may be constructed. Since the horizon length $2h$ is about 1000 m, it is expected that for grids with manageable sizes, using the standard floating point representation with single precision will not introduce oscillations.

5.7 Conclusions

An analysis has been carried out to avoid numerical problems in the final algorithm. Oscillating solutions may appear despite established stability and convergence properties of the discretization method. The interplay between the objective and the errors is crucial. An error in the velocity state correspond to an error in kinetic energy and it may lead to that the algorithm erroneously finds a solution different from the true optimum. The analysis in Section 5.6 gives, even though simplified, understanding into what measures to take. The results are as follows. Regarding discretization errors, it was shown that the Euler backward method or the trapezoidal rule is preferred over the Euler forward method for the test problem. For the more complex prediction model, the example in Figure 5.2 shows that undesired solutions are avoided if an appropriate method is used. Concerning state errors, the bound (5.45) estimates the amount of perturbation of a velocity state allowed for the test problem. This bound is used in the inverse approach when the cost-to-go must be approximated. The example with the prediction model in Figure 5.3 shows that unwanted solutions is prevented by the use of the bound.

The outcome of this chapter is a well performing dynamic programming algorithm. The complexity is lowered by a preprocessing algorithm that reduces the search space prior to the optimization. Besides the standard approach, an inverse approach for the evaluation of the core functional equation is formulated. By using a proposed fast search method combined with this approach, it would be possible to reduce the complexity further. The method chosen for the coming evaluation of the algorithm is the inverse approach.

6

Evaluation Setup

The look-ahead control strategy has been evaluated in both simulations and experiments. In this chapter, the equipment used and the basis for the parameters in the model and in the algorithm will be described. Further, the realization of the experimental and simulation environments are explained. The estimation of the road slope for the trial route is also briefly described.

6.1 Vehicle

The truck simulated and used in the experiments is a SCANIA tractor and semi-trailer. The specifications of the experimental vehicle are given in Table 6.1.

Figure 6.1: A SCANIA tractor and trailer.

Component	Type	Characteristics
Engine	DC9	cylinders: 5
		displacement: 9 dm^3
		max.torque: 1,550 Nm
		max.power: 310 Hp
Gearbox	GRS890R	12 gears
Vehicle	-	total weight: 39,410 kg

Table 6.1: Truck specifications.

The truck has a relatively small engine displacement in comparison to the total vehicle weight. This was a deliberate choice with the intention that the road slope should make noticeably influence the motion of the vehicle.

The only parameter in the prediction model, see Section 3.1.11, that is identified from measured data is the mass. The tractor and semi-trailer were weighed before the experiments. Other parameters were set from e.g. data sheets.

6.2 Algorithm Parameters

The algorithm parameters are presented in Table 6.2. The verbal interpretation of these parameters is that the controller will look ahead 1500 m at the road slope and optimize the velocity trajectory in the interval from 79 km/h to 89 km/h. The horizon is divided into 30 steps of 50 m and the velocity state space grid in the optimization has a resolution of 0.2 km/h.

Parameter	Function	Value
h	Step length	50 m
N	Number of steps	30
$h \cdot N$	Horizon	1500 m
δ	Velocity discretization	0.2 km/h
v_{min}	Min. allowed vel.	79 km/h
v_{max}	Max. allowed vel.	89 km/h

Table 6.2: User parameters.

Alongside the conventional cruise controller, the truck is equipped with a brake controller. The system is activated when the truck velocity reaches above a certain offset from the cruise controller set speed. In the experiments, it was assured that this limit was the same for each pair of runs that was to be compared.

The chosen penalty factors are shown in Table 6.3. The trade off between fuel and time use is done by calculating a value of β in order to receive a stationary solution in the middle of the desired velocity interval, that is 84 km/h. The

magnitudes of the fuel term and time term in the cost function (5.11) are about 10^{-1} and 10^{0} respectively with current parameters. The smoothing term a_k has a magnitude of about 10^{-1}. The size of the factor γ is chosen for smoothing but still such that this term becomes considerable smaller than the others. The parameter ϑ for damping gear shifts is not used since the shifting is not

Factor	Penalizes	Value
	Fuel use	1.0
β	Time use	6.2
γ	Velocity changes	0.1

Table 6.3: Penalty factors.

optimized. Instead a model of the automated manual transmission is taken into account in the optimization. This is further explained in Section 6.3.1.

6.3 The Experiment Vehicle

The information flow in the experimental setup is shown schematically in Figure 6.2. The coordinates from a GPS receiver are matched against a stored road

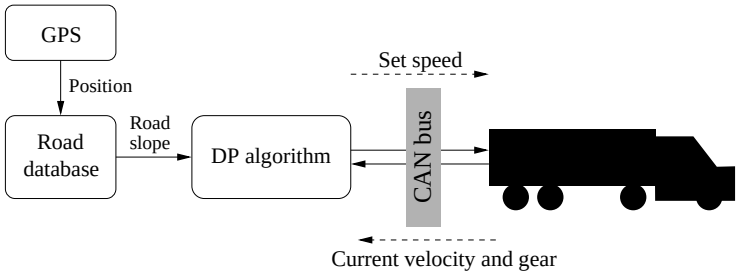

Figure 6.2: Information flow overview.

database from where the slope along the current horizon can be extracted and fed to the algorithm. The algorithm receives the current velocity and gear, and sends set speeds to the cruise controller via the CAN bus. The cruise controller is thus an inner loop that determines the actual fueling level. The outer loop, the optimization algorithm, feeds the inner loop with new set points.

A robust inner loop is needed which can follow the algorithm output in an acceptable way. Open loop control will, for example, not be able to keep a constant speed on level road if the estimate of the vehicle mass is inaccurate. Using a structure with a cruise controller, which has been proved to be robust, as an inner loop has apparent advantages considering model errors and disturbances.

The software needed for the controller is implemented in C++ on a portable computer. The laptop has an Intel Centrino Duo 1.20 GHz processor and 1 GB

RAM. An overview of the implementation is given in Figure 6.3. With the used algorithm parameters, a solution is calculated in tenths of a second on this computer. A number of software modules are designed for different tasks, see

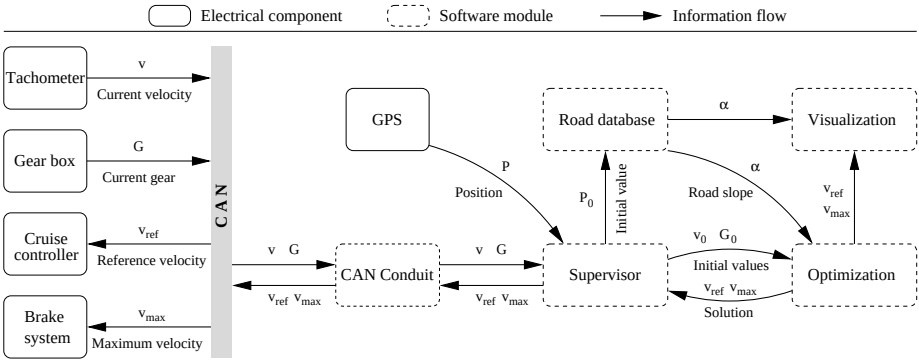

Figure 6.3: Implementation overview.

Table 6.4. The modules run as independent processes and communicate with each other by shared memory. Signals are received and transmitted to a number of components in the truck. The current velocity is measured with a tachometer and the current gear is reported by the gear box. The cruise controller is fed with the optimal set point and the maximum allowed velocity is sent to the brake system. A GPS receiver gives the coordinates for the current position. Although only the first sample of the solution is used for control, the optimal solution for the entire horizon is saved with the purpose to graphically show the solution on the laptop. The visualization module updates a window with the optimal velocity trajectory and the predicted gear every time the algorithm outputs a new solution. The estimated road slope along the look-ahead horizon is also integrated and shown together with the solution.

Module	Purpose
CAN Conduit	handles CAN communication
Optimization	implements the fuel-optimal algorithm
Road database	extracts slopes ahead of the current position
Supervisor	acts as the central node for the system
Visualization	graphically displays the solution on the laptop

Table 6.4: Description of software modules.

Two views from inside the truck are portrayed in Figure 6.4. One computer, seen to the left, was used to log data from control units in the truck. A second computer, seen to the right, run the described software modules. Two GPS receivers were used. One cheaper unit (about $100) provided the algorithm with a position at 4 Hz for the purpose of matching the position against the

stored road database and extracting the slope along the look-ahead horizon. Another unit (about $1000) provided the log computer with a position at 20 Hz enabling all vehicle data to be logged together with the current coordinates.

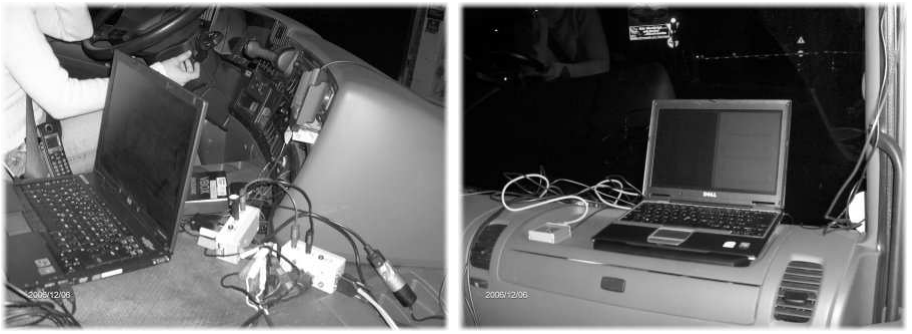

Figure 6.4: Views from the passenger seat inside the truck. Left: The computer used for collecting data from the control units in the vehicle. Right: The computer running the optimization algorithm and the accompanying software modules.

6.3.1 Adjustments for the Experiments

Some adaptations of the control strategy were made with respect to the transmission and cruise controller of the experimental vehicle.

Gear Shift Prediction

The algorithm controls the vehicle by adjusting the set speed sent to the conventional cruise controller, as depicted in Figure 6.2. The existing cruise controller is already prepared to receive and handle set points from other control units. This is for example the case in adaptive cruise controller systems. For the gear box, this is however not yet the case. Therefore, it was decided not to control the gear selection. Gear shifting is instead fully controlled by the existing system for automatic gear shifting of manual gearboxes. This is handled in the optimization algorithm by making a simple model of the shift control system and taking it into account when calculating transition costs.

The gear shift prediction model simply consists of tabulated values of gear number and two engine speed threshold values. If the lower threshold is reached on the corresponding gear, a shift to the next lower gear is predicted. Likewise, the upper threshold determines the point of a shift to the next higher gear. This model of the automatic shift system, in spite of the crude nature, demonstrated to have satisfactory performance, as will be seen in Section 7.1.

In the optimization algorithm, a shift that is not predicted is assigned an infinite cost. Due to this large penalty, shifts which are not possible outputs

from the prediction model will not be part of the solution.

Improving Cruise Controller Tracking

Before the trial runs, drives were made merely to test the system functionality. In these runs, it was noticed that the velocity trajectory given from the optimization was poorly effectuated. The existing cruise controller did not respond well to the small changes of the set point between consecutive samples. The cruise controller is primarily designed to keep a constant speed and also to give a comfortable acceleration when for example resuming to a previous set point. The controller is however not designed to track a trajectory such as the output from the algorithm. The solution trajectory will at most change as much as the maximum acceleration (or minimum deceleration) given by the prediction model. In this experiment, a step length of 50 m was used. The maximum possible change in the velocity over this length together with present signal noise evidently makes it hard for the existing cruise controller to effectuate the optimal solution.

To tackle this problem, simple ad-hoc rules were set to increase or decrease the set point, more than the given by the actual solution, in certain situations. By studying the fueling level for a number of samples of the solution, it is guessed whether a large acceleration or deceleration is wanted. The rules are verbally stated as follows.

Torque mode If the mean value of the fueling level for the next R samples is above a set threshold, increase the set point to the upper optimization bound.

Drag mode If the mean value of the fueling level is below a set threshold for the next R samples, decrease the set point to the lower optimization bound.

The rules worked rather well as will be demonstrated by experimental results in Chapter 8. It is also possible to model the cruise controller and take the inverse model into account in order to improve the response but then the algorithm complexity would increase. Another way to remedy the tracking problem could be a cruise controller design where the desired acceleration can be given as input.

6.4 The Simulation Environment

The evaluation model described in Section 3.1.12 is implemented in MATLAB SIMULINK and interfaces to the algorithm code are created. Owing to these interfaces, exactly the same algorithm code are used in the simulation environment as in the experiments. The implementation uses templates from the Center for Automotive Propulsion Simulation (Eriksson et al., 2004).

6.5 Road Database

The trial route is a segment of about 120 km on the highway E4 in Sweden between the cities of Södertälje and Norrköping.

The slope in front of the vehicle for the length of the look-ahead horizon is needed to be known in advance. For this reason, the road slope along the trial route is estimated off line prior to the experiments. This is done by aid of a non-stationary forward-backward Kalman filter (Hellström et al., 2007; Sahlholm et al., 2007). The measurements were obtained at 20 Hz from a GPS unit. The filter inputs are vertical and horizontal velocity of the vehicle, altitude and the number of reachable GPS satellites.

The estimated slope and calculated altitude are shown in Figure 6.5. The slope is rather moderate. It ranges from -4% to +4% but is mostly in between about -2% to 2%.

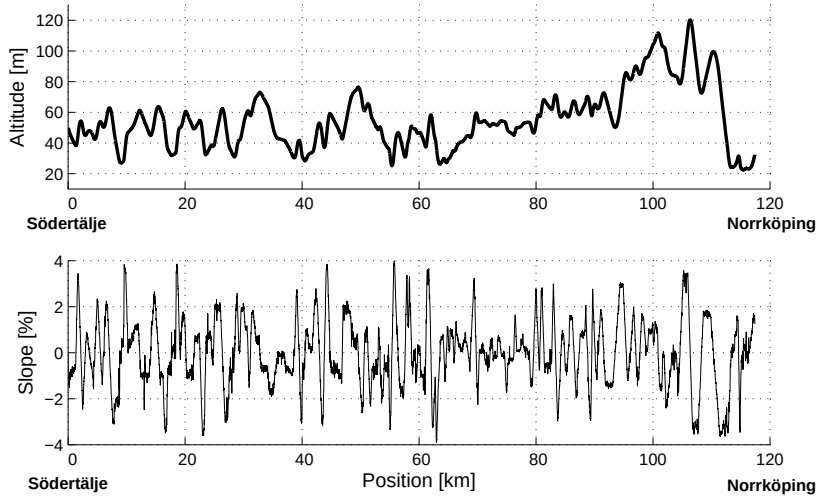

Figure 6.5: Estimated road slope and calculated altitude along the trial route. The route is the highway E4 between the cities of Södertälje and Norrköping.

The position is measured by a GPS unit and after the closest position that is stored in the database is found, the slope values ahead of the vehicle are extracted.

6.5.1 Road Segments

In the coming chapters, it will be interesting to study truck behavior in more detail. For that purpose representative road segments have been chosen. An overview of the segments are given in Figure 6.6. The start of a road segment is marked with a circle and the end with a cross.

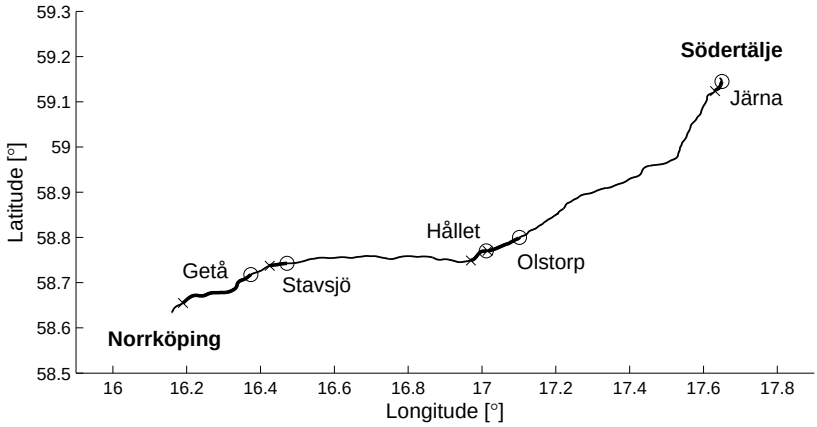

Figure 6.6: For detailed studies a number of road segments along the trial route have been selected and named. The bounds of a segment are marked with a circle and a cross. Coordinates are given in decimal degrees.

To study controller characteristics in detail, two segments have been chosen. The first is a 2.5 km segment close to Södertälje and is named *the Järna segment*, see e.g. Figure 7.6. The second one is a 3.5 km segment about halfway on the trial route and called *the Hållet segment*, see e.g. Figure 7.5.

For validation purposes two segments have been used. The first is the Hållet segment. The second one is 6 km just before the Hållet segment and called *the Olstorp segment*, see Figure 7.1. These segments are both close to the city of Nyköping that is situated about halfway between Södertälje and Norrköping.

In order to study the rolling horizon used by the controller, three segments have been used. The first two are the Järna and the Hållet segments. The last one is a 2.5 km segment close to Norrköping labeled *the Stavsjö segment*, see Figure 8.7. To study gear shifting strategies a 14 km segment close to the Stavsjö segment is selected and named *the Getå segment*, see Figure 7.12.

7

Model Validation and Parameter Studies

The model based control in this work uses a model to predict vehicle motion and energy consumption. The validity of this model will be investigated by comparing its predictions with measurements. To evaluate the potential of look-ahead control, simulations are carried out to predict performance in terms of overall impact on fuel consumption and travel time as well as detailed controller behavior. Comparison of these results with the experimental results obtained gives an indication on the accuracy to expect from such simulation results. Simulations are well suited for parameter studies. The influence of a number of parameters on the solution will be investigated through simulations using the setup and parameters described in Chapter 6.

Whenever reviewing a vehicle control strategy claiming to save energy, the trip time must be considered in combination with stated fuel consumption numbers. There is no challenge in saving fuel by traveling slower. For a convincing result on controller performance, the fuel use must be lowered without increasing the trip time in comparison with the used measure.

7.1 Prediction Model Validity

The performance of the simple prediction model is investigated by comparing measured data and offline simulations. The measured control signals fueling, braking and gear together with estimated road slope are used as inputs to the prediction model. The output, acceleration and fuel flow, are integrated and compared to the measured velocity and fuel use. The measured velocity is also used as input to the prediction model for gear selection and the output is

compared to the actual gear used. The data that are used come from drives with the cruise controller active, and were recorded at about the same time of day on two consecutive days. The road segments in the coming figures are the Olstorp and the Hållet segments, see Section 6.5.1.

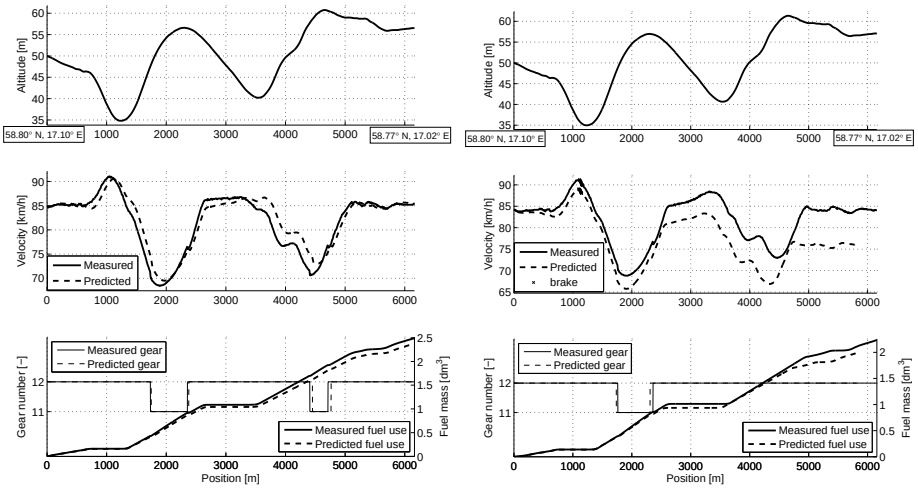

Figure 7.1: The Olstorp segment. The absolute prediction error becomes large, especially in the right figure. Still, the dynamic response to the control and road slope is captured acceptably.

In Figure 7.1 the Olstorp segment is shown. The velocity prediction performs significantly better in the left figure. The absolute error becomes large in the right figure. Still, the influence of the varying road slope on the predicted acceleration is seen to be generally satisfactory. The prediction of the gear selection is rather good with the exception of the shift at 4.5 km in the left figure which is not predicted to occur at all. Comparing the measured data on the segment between 2.5 km and 3.5 km in the left and right figures are interesting. The fuel use curve reveals that the fueling is zero. In the left figure the truck keeps about the same velocity while in the right figure, the truck accelerates. Between 500 m and 1100 m there is also a segment with zero fueling. In this segment, the difference in the acceleration is not as large. Since it does not seem to be a general trend comparing the two drives, the cause could for example be a transient increase of the load from air drag or an auxiliary device. However, no certain conclusion can be drawn from the recorded data on what the cause of this is. The prediction model does not capture these effects, but the trends in the velocity are yet captured well after 3 km in the right figure, although the absolute value has drifted away.

Figure 7.2 shows the Hållet segment. The gear selection is predicted well. By visual inspection, it is seen that the sum of the errors in the prediction of velocity is about the same in the left and right figure. In both runs, it is

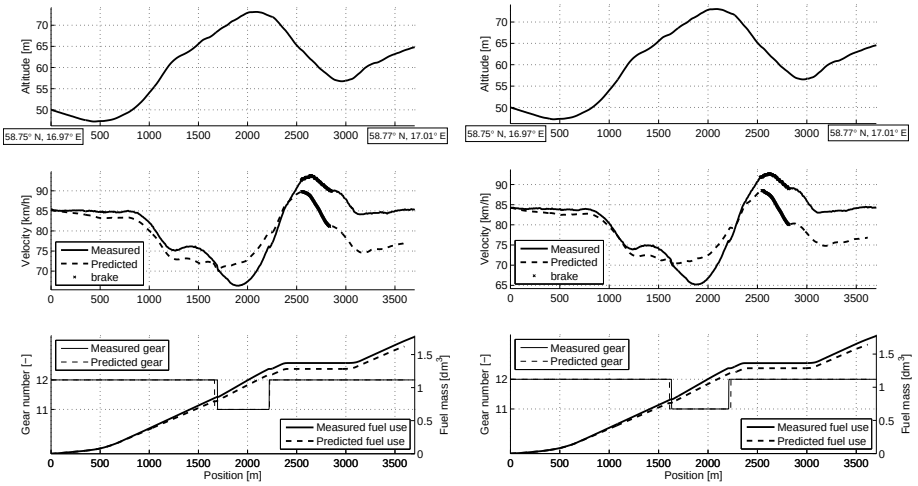

Figure 7.2: The Hållet segment. The predictions are poor about the midsection and this suggests that the slope might be badly estimated here.

apparent that there is a negative prediction error at first and a large positive error around 2 km. The positive and negative accelerations around 1.5 km are poorly captured. In the previous figure it was seen that the influence of the road slope was captured rather well. Since this is not the case here, it suggests that the slope might be crudely estimated.

The prediction model is rather simple. The data presented in this section indicate that changes from one drive to another can notably influence the absolute prediction performance. One way to enhance performance could be to identify model parameters online. Further, the prediction naturally relies heavily on estimated vehicle mass and estimated road slope. The vehicle mass is however expected to be estimated accurately since the entire vehicle was weighed. The quality of the road slope information relies on the estimation method but is hard to evaluate since there is no recognized and accurate source of information about the true road topography. The important property of the prediction model is however to be able to accurately estimate the energy consumption of one control signal trajectory relative to another. Therefore, the principle effects on vehicle motion and fuel consumption from control signals and road slope should be well captured.

It should finally be noted that the prediction horizon used in the optimization is 1.5 km and thus much shorter than the distances in these validations. The horizon is one fourth of the distance in Figure 7.1 and about half the distance in Figure 7.2.

7.2 Performance Prediction

An interesting question is how accurate simulation studies are in their assessments. With careful modeling and evaluation, the fuel consumption of a heavy truck can be predicted with an error of a few percent (Sandberg, 2001b). However, when evaluating control strategies the absolute accuracy is of less importance as long as the relative impact on the objectives due to different strategies can be judged well. In the present application, the relative change in time and fuel use is thus of main interest. A simulation environment is used with the same setup as in the experiments. This facilitates comparisons between the predicted performance through the simulation environment and actual performance obtained on the road, see Chapter 8. .

7.2.1 Overall Results

A number of simulations are undertaken in order to compare the fuel consumption of the conventional cruise controller (CC) and the look-ahead controller. The algorithm parameters are held constant and only the CC set speed is varied.

The results in Figure 7.3 show that a CC set speed of about 85 km/h will render the same trip time as with the look-ahead controller. The overall results

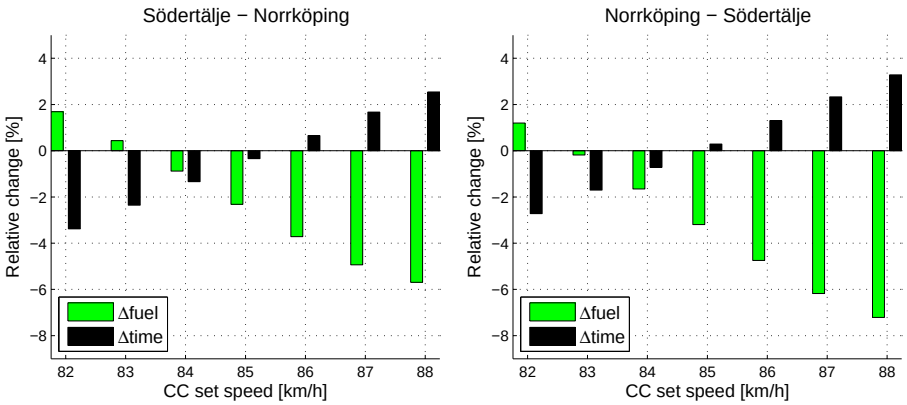

Figure 7.3: Simulated look-ahead control performance compared to ordinary cruise control with varying set speed.

with this set speed are shown in Figure 7.4. These are calculated as the average of the values in both directions. For these mean values, the look-ahead controller lowers the fuel consumption with almost three percent without increasing the trip time traveling back and forth. Studying the simulations in further detail also reveals that the simulated number of gearshifts is reduced notably in both directions. Although the shifts were not controlled directly, the look-ahead algorithm evidently affected the shifts indirectly.

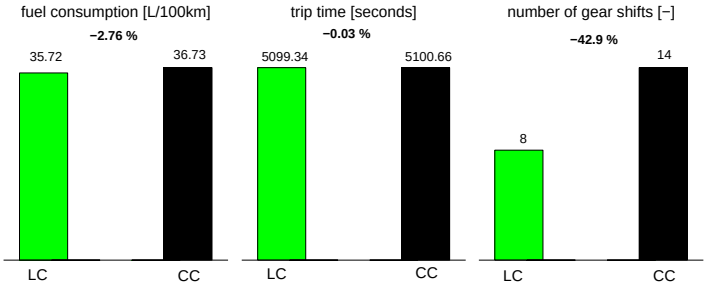

Figure 7.4: Simulated results showing potential for fuel saving and a reduction of the number of gear shifts.

7.2.2 Control Characteristics

The controller behavior will now be examined in detail for a number of selected road segments along the trial route. These are the Järna and the Hållet segments, see Section 6.5.1. The same segments are used in Chapter 8 for evaluating the actual behavior achieved in the on-road experiments.

The figures, see e.g. Figure 7.5, have four sub-figures and all data are displayed with position as the horizontal axis. The road topography is shown at the top. The second sub figure shows the simulated velocity for the look-ahead controller (LC) and the standard cruise controller (CC). The third part shows normalized fueling (thick lines) and brake levels (thin lines). The last part displays both the engaged gear number and the accumulated fuel use. Data connected to the simulation of the LC is displayed in solid lines and data associated with the CC is displayed with dashed lines in these figures. The simulated travel time and fuel use on the segment are shown together with the relative change (Δfuel,Δtime) above the top figure. A negative value means that the value is lowered by the look-ahead controller. Note that the relative changes on these short segments of a few kilometers are not comparable to the results on the entire route which ranges more than 100 km.

The Hållet Segment

Figure 7.5 shows simulations on the Hållet segment. In the left figure, at 500 m it is seen that the LC accelerates prior to the uphill that begins at 750 m. This avoids the gear shift that the CC is forced to, and leads to a higher velocity climbing the hill up to 1750 m. At the top of the hill at 1750 m, the LC slows down in contrast to the CC. The truck is thus let to accelerate by the slope. The CC will however use a non-zero fueling as long as the truck is going slower than the set point. The slow-down reduces the need for braking later in the downslope and thereby the inherent waste of energy is lessened. From the fuel integral at the bottom, it is seen that the LC consumes more fuel the first 1.5 km owing to the acceleration. However, in total less fuel is spent by the LC due to

the slow-down at the top of the hill.

Simulating the other direction, see the right half of Figure 7.5, gives similar features. A gain of speed at 250 m and then a slow-down at the top of the hill at 2250 m. In both directions, time as well as fuel are saved.

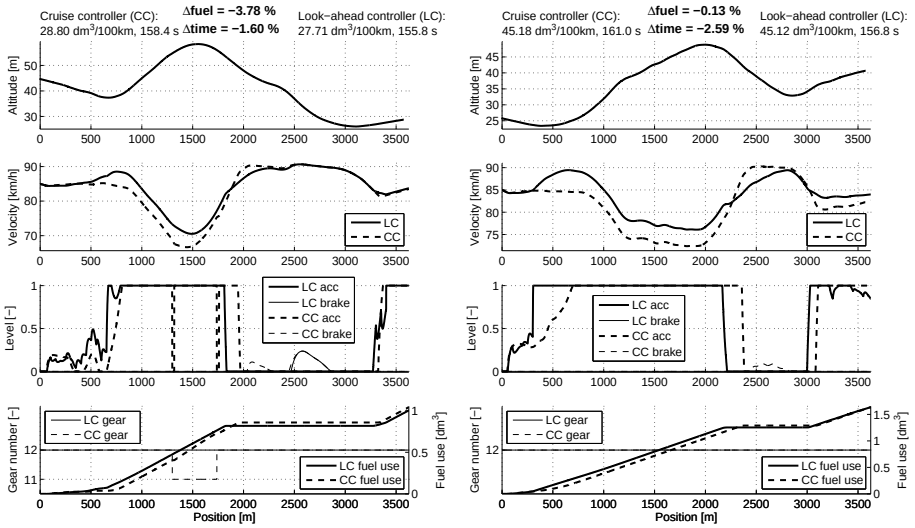

Figure 7.5: Simulation on the Hållet segment. Left: The LC accelerates at 500 m prior to the uphill thereby avoiding a gear shift. At 1750 m the LC slows down and the truck is let to accelerate in the downslope. Right: Similar characteristics are seen with an acceleration at 250 m and a slow-down at 2250 m.

The Järna Segment

In Figure 7.6, simulations on the Järna segment are shown. The left figure show that the LC begins to gain speed at 200 m, before the uphill begins at 400 m. At 1300 m, the LC slows down and lets the truck accelerate in the downslope. In total, the LC uses more fuel but travels faster than the CC on this segment.

In the right half of Figure 7.6 a simulated drive in the other direction is shown. The LC slows down at 1400 m and thereby avoids the braking that the CC is forced to at about 2000 m.

7.3 Parameter Evaluation

It is of interest to study the influence of horizon length, gear shifting strategy, neutral gear, cruising speed and vehicle mass on principle behavior. The impact of these parameters on the fuel consumption and travel time will be evaluated through simulations in the following sections.

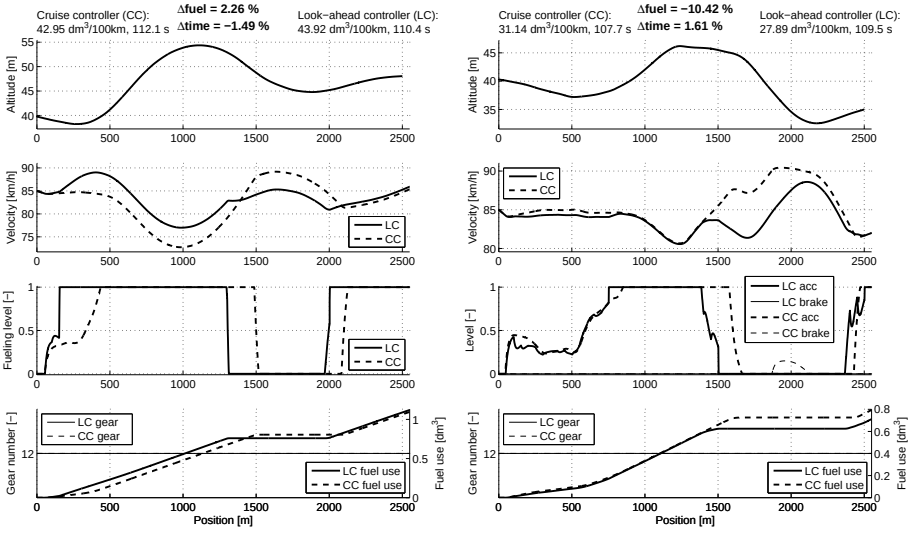

Figure 7.6: Simulation on the Järna segment. Left: The LC gains speed at 200 m prior to the uphill and slows down at 1300 m and the truck is let to accelerate in the downslope. Right: The LC slows down at 1400 m thereby avoids braking later on.

7.3.1 Mass

The vehicle mass in relation to the available engine power is one important influencing factor on the nature of the present problem. To study this, simulations are made with varying mass, and the fuel consumption and travel time are compared. In these simulations the cruise controller (CC) set speed was adjusted in order to make the change in travel time small. The results are shown in Figure 7.7.

The potential of look-ahead information is evidently dependent on the vehicle mass considering other model parameters constant. This is expected since the mass will determine the effect the road slope will have on vehicle motion. The results should be dependent on the road topography as well. For example, on a more difficult route where significant slopes are more frequent it is expected that the range of vehicle masses where there is evident potential would be larger.

7.3.2 Set Speed

The cruising speed is chosen to be around 84 km/h in most of the simulations in this chapter. To suggest the significance of this choice, the simulations in Section 7.2.1 are repeated at other cruising levels.

Regarding the optimization parameters, the allowed velocity interval is low-

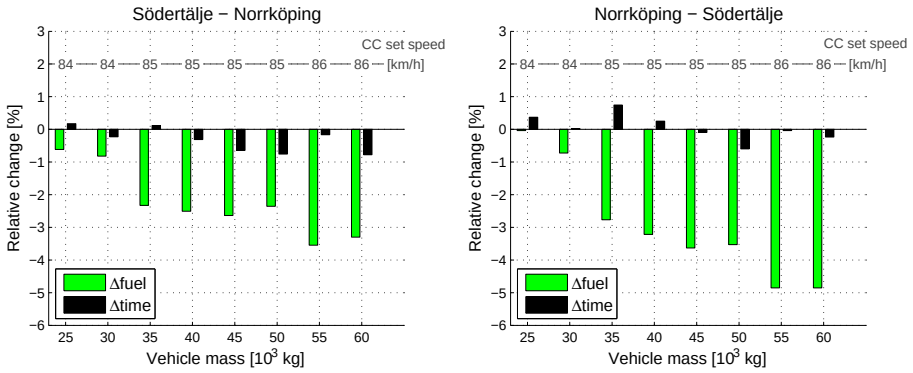

Figure 7.7: Simulations with varying mass. The cruise controller (CC) set speed has been adjusted as to make the change in travel time small.

ered from [79,89] to [69,79] [km/h] and the penalty parameter β is chosen to 4.3 in order to receive a stationary solution in the middle of the new velocity interval, that is 74 km/h.

These new algorithm parameters are held constant and the cruise controller (CC) set speed is then varied. The trip time with the cruise controller will vary with the set point and the resulting fuel consumption can be compared to the one obtained with the look-ahead controller. The results are shown in Figure 7.8. According to the figure, a CC set speed of about 74 km/h should

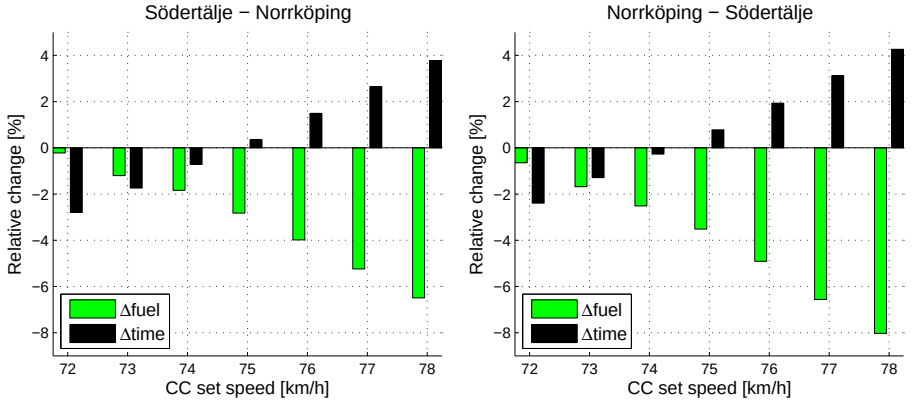

Figure 7.8: Simulated performance compared to ordinary cruise control with varying set speed with another velocity interval.

yield the same trip time as with the look-ahead controller.

Comparing Figure 7.8 with the previous results in Figure 7.3 reveals that the potential of look-ahead control is about the same for the respective velocity intervals.

7.3.3 Horizon

The length of the look-ahead horizon determines how far the information about the upcoming road topography reaches. The division of the horizon into a number of steps determines the position resolution of this information. Since adding more information means an increased algorithm complexity a trade off is made. In this section the impact on algorithm performance due to the horizon length is investigated. The step size is held at 50 m and the number of steps is varied to obtain different horizon lengths.

In Section 7.2 the controller performance is predicted in terms of the impact on the fuel consumption and travel time on the trial route. Those simulations do not optimize gear shifts since only shifts predicted by the model are allowed. Unlike those, the simulations here will optimize gear shifts.

Simulation results are shown in Figure 7.9. The fuel consumption is reduced with about two to three percent while keeping about the same trip time. In the direction towards Norrköping the best results are obtained with an horizon of more than 750 m. In the other direction, a horizon longer than 1000 m is required.

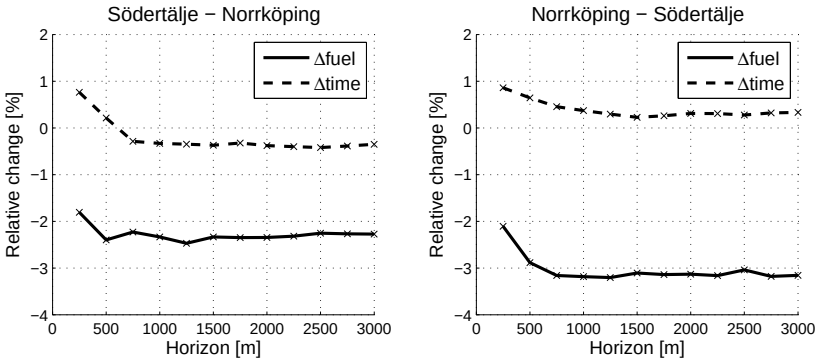

Figure 7.9: Simulations with varying horizon length with optimized gear shifts.

7.3.4 Gear Shifts

Gear selection was not controlled directly by the look-ahead controller in the experiments, as mentioned in Chapter 6. A model of the automatic gear shifting system is instead taken into account. The impact on the performance of this restriction will now be studied. For this reason, the varying horizon simulations from Section 7.3.3 are repeated with the change that the prediction model of the automatic gear shift system is taken into account. Adding another degree of freedom to an optimization problem should at least give the same solution but hopefully a better solution, that is a lower objective value in a minimization problem. The results from simulations are shown in Figure 7.10 that should be

compared to Figure 7.9. Comparing the figures reveals that the improvement is rather small. The gain of optimizing gear shifts with the current setup on this route thus seems low. It should be noted that the route reflects highway

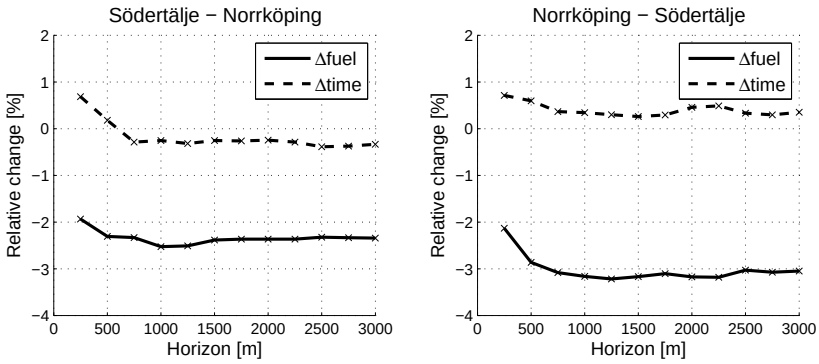

Figure 7.10: Simulations with varying horizon length without optimizing gear shifts.

driving with relatively few gear shifts. Simulations of the evaluation model with standard cruise control indicated about 14 shifts in either direction of the 120 km route with the current setup according to Section 7.2.1. This indicates the number of sections where differences in the control with and without optimized gear shifts probably appears. Due to the rather low number of shifts compared to the route length, small changes in the objectives are expected.

Since it is generally fuel efficient to have the highest applicable gear engaged, a down-shift will probably occur only when it is unavoidable. With look-ahead information down-shifts may be avoided or the position of the shifts changed in comparison to a system with no look-ahead. For short but significant uphills, a shift may be avoided by gaining speed prior to the hill. The shift points may be moved such that a down-shift is made in advance when a difficult segment approaches or that a lower gear is kept if there are more uphills ahead.

7.3.5 Neutral Gear

The use of neutral gear to reduce fuel consumption is one interesting approach. Computer simulation results (Fröberg et al., 2005; Hellström et al., 2006) have indicated that there is a possible potential and there are also commercially available transmissions (Volvo press release, 2006) with integrated logic that aims at a reduced fuel consumption by the use neutral gear.

The possible potential of using neutral gear will now be studied. The simulations with varying horizon from Section 7.3.3 are therefore repeated with the change that neutral gear is an allowed control in the algorithm. Allowing neutral gear adds another degree of freedom to the optimization problem and should therefore give the same solution or a better one with regard to the

current objectives. The gain is shown by comparing the simulation results in

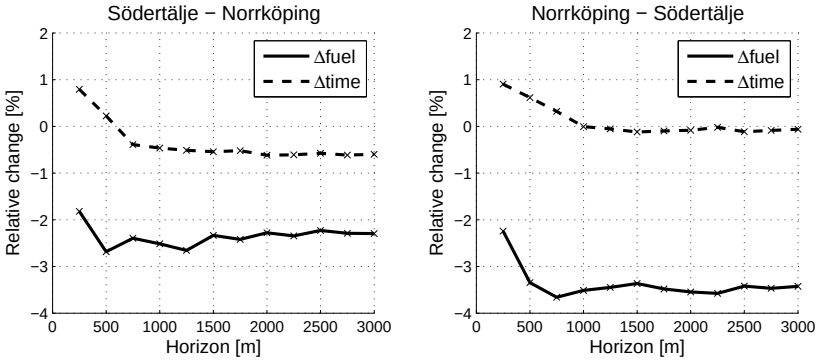

Figure 7.11: Simulations with varying horizon length with optimized gear shifts including neutral gear.

Figure 7.11 with the previous results in Figure 7.9. The fuel consumption and the travel time reduction is slightly reduced. The change that appears in the direction towards Södertälje is somewhat more apparent.

It has been noted when performing these simulations that the results are rather sensitive to the modeling of the idle fuel flow and the shift process.

7.4 Shifting Strategies

In order to illustrate shifting behavior the Getå segment is used, see Section 6.5.1. The allowed velocity interval is set to [69,79]. The penalty parameter β is chosen to 4.3 in order to obtain a stationary solution of 74 km/h. The results are shown in Figure 7.12 where the left part comes from a simulation with optimized gear shift and the right part is the result without gear shift optimization. The positions at which the shifts are made are moved slightly. The most evident difference occurs around 2 km where the optimized sequence holds gear 12 for about 200 m extra and then directly shifts into gear 10. The non-optimized sequence arrives at the same gear at about 2300 m but through two shifts. In Section 7.3.4 it was shown that the optimization of gear shifts did not give a significant improvement in terms of fuel and time use on the trial route. However, the shifting behavior is influenced which can increase the maximum slope that can be handled without driver intervention and improve the driver comfort.

7.5 Conclusions

The validation of the prediction model shows that the dynamical response to control and road slope variations is good in general. There are some effects that

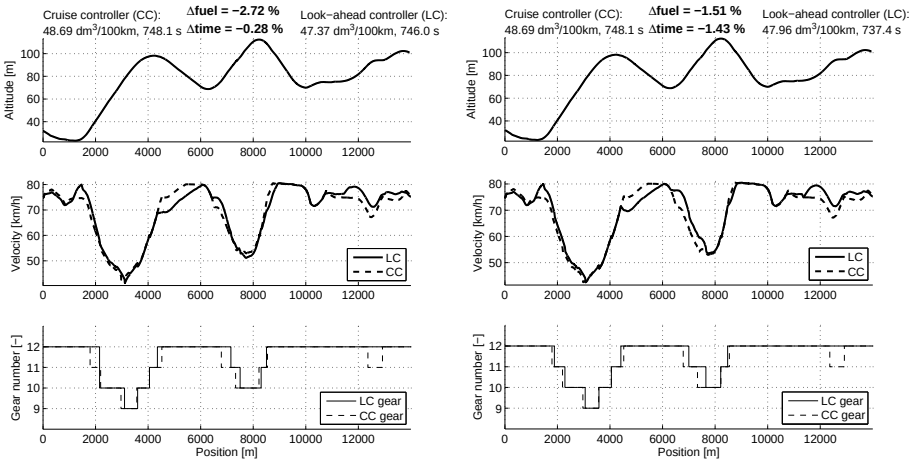

Figure 7.12: Simulation on the Getå segment. The optimized gear trajectory(to the left) shifts at slightly different positions compared to the non-optimized trajectory (to the right). This is most evident around 2 km.

are not captured by the simple model, but since it is used in the optimization the complexity should be kept low, and it performs quite satisfactory.

Simulations show that with the chosen setup, the fuel consumption can be reduced with almost three percent on the trial route without increasing the travel time and the number of gear shifts is reduced significantly. The dependency on vehicle mass shows an interesting behavior, see Figure 7.7. With other parameters fixed there are notable increases in fuel gain for larger masses. When the velocity interval considered for optimization was lowered with 10 km/h it was discovered that the potential for fuel saving still were about the same. By varying the horizon length, it was shown that a look-ahead horizon of about 1000 m or more gave the best results. A longer horizon length was shown not to give noticeable improvements.

8

Experimental Results

Trial runs has been performed on a segment of about 120 km on the highway E4 in Sweden between the cities of Södertälje and Norrköping. The experiments were carried out in collaboration with SCANIA. In this chapter, the performance of the look-ahead controller is examined by demonstrating overall impact on fuel consumption, time use and shifting behavior as well as detailed controller characteristics. The setup for the experiments is explained in Chapter 6. Vehicle specifications are given in Table 6.1 and algorithm parameters are given in Table 6.2 and 6.3.

8.1 Performance

In total, five comparative trial runs were made. Each run consisted of one drive with look-ahead control and one with standard cruise control in a direction on the road from Södertälje to Norrköping. The algorithm parameters were the same for all runs. The trip time will then become about the same for all drives with the look-ahead control. The set point for the cruise controller was chosen in order to achieve a trip time close to the one obtained with look ahead. The set points used are stated in Table 8.1. In the table some notes about the weather and road conditions are also given to provide a sketchy picture of the situation. Further, the traffic was light to moderate during the experiments. The experiment in November was only performed in the direction from Södertälje and Norrköping whereas the other experiments were performed in both directions each day.

Date	Weather	Road	CC set speed
1 Nov. -06	0.5°C, rainy, windy	wet	86 km/h
11 Dec. -06	5°C, some rain, windy	wet	85 km/h
12 Dec. -06	5°C, calm	wet	84 km/h

Table 8.1: Trial run setting. Weather notes give a rough idea of the conditions.

8.1.1 Overall Results

The relative change in fuel consumption and trip time (Δfuel,Δtime) are shown in Figure 8.1 for each direction on the trial road. A negative value means that the look-ahead controller (LC) has lowered the corresponding value. The set point for the cruise controller (CC) increases along the horizontal axis. The left-most result is maybe the most convincing since it reduces fuel use and trip time in both directions.

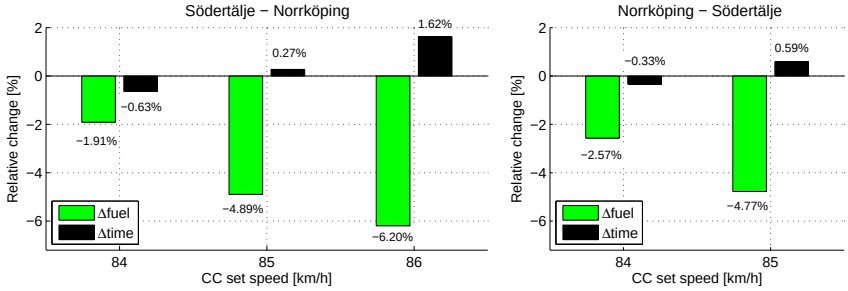

Figure 8.1: Relative changes in fuel consumption (Δfuel) and trip time (Δtime) obtained in the trial run. The set point for the cruise controller (CC) is varied in the experiments and increases along the horizontal axis.

In Figure 8.2 the overall results are shown. These are calculated as the average of the values obtained with the experiments made in December, where drives in both directions of the trial road were made on each day. The results thus entails four runs back and forth on the trial road, two runs with the CC and two with the LC. For these mean values the fuel consumption was lowered with 3.53%, from 36.33 L/100km to 35.03 L/100km, with a negligible reduction of the trip time (0.03%) in comparison with the CC. Also interesting to note is that the mean number of gear shifts on this route decreases from 20 to 12 with the LC. By accelerating before significant uphills some shifts are avoided by the LC as will be seen in the detailed figures in the following sections. The controller behavior has been appreciated as comfortable and natural by participating drivers and passengers.

The fuel consumption results in Figure 8.2 agrees well with the values obtained in simulations, see Figure 7.4 (p. 59). The simulated trip time is about 3 min longer but this is partly due to that the simulations are done over a

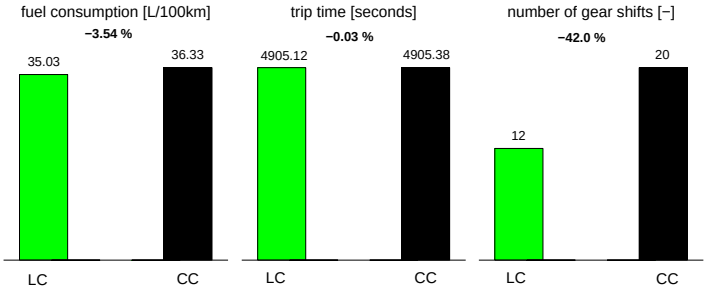

Figure 8.2: Overall results showing a fuel saving potential of about 3.5% without an increased trip time. The mean number of gear shifts is also notably reduced.

longer distance than in the measurements. The predicted number of gear shifts are considerably underestimated but the relative decrease of gear shifts due to look-ahead control is well captured. The relative change for the other measures agrees rather well with the simulations.

8.1.2 Control Characteristics

With the intention to give a representative demonstration of controller characteristics in detail two road segments have been chosen. These are the Järna and the Hållet segments, see Section 6.5.1. Data from the trial runs on these segments, in each direction, will be presented. In Chapter 7, the controller behavior was simulated on the same set of road segments.

In agreement with the corresponding figures in Chapter 7, each figure is divided into four sub-figures, see e.g. Figure 8.3, all having the position as the horizontal axis. The road topography is shown at the top and the coordinates for the start and final position are also given on the horizontal axis. The next subfigure shows the velocity trajectories for the look-ahead controller (LC) and the standard cruise controller (CC). The third part shows normalized fueling (acc) and retarder (brake) levels with thick and thin lines respectively. At the bottom, both the engaged gear number and the fuel use are shown. Data related to the LC is displayed in solid lines and data associated to the CC is displayed with dashed lines in these figures. Above the figures, the time and fuel spent on the section are shown together with the relative change (Δfuel,Δtime) in these values between the two controllers. A negative value means that the value is lowered by the look-ahead controller.

The Hållet Segment

Figure 8.3 shows the Hållet segment. The corresponding simulation is shown in Figure 7.5 (p. 60). In the left figure, as in the simulation, the LC accelerates at 500 m prior to the uphill and slows down at the top of the hill at 1750 m

in comparison to the CC. In contrast, the simulated results show that the LC avoids the gear shift but this is not the case in this measurement.

The trip in the other direction is shown in the right half of Figure 8.3 and Figure 7.5. Similar features are seen again. A gain of speed at 250 m and then a slow-down at the top of the hill at 2250 m. The gear shifts around 2 km do however not appear in the simulated trip. In the measurements, both controllers reach a lower velocity around the top of the hill compared to the simulations which explain this discrepancy.

In both directions, time as well as fuel are saved. The absolute values of measured and simulated fuel and time use are close but the relative changes differ more clearly.

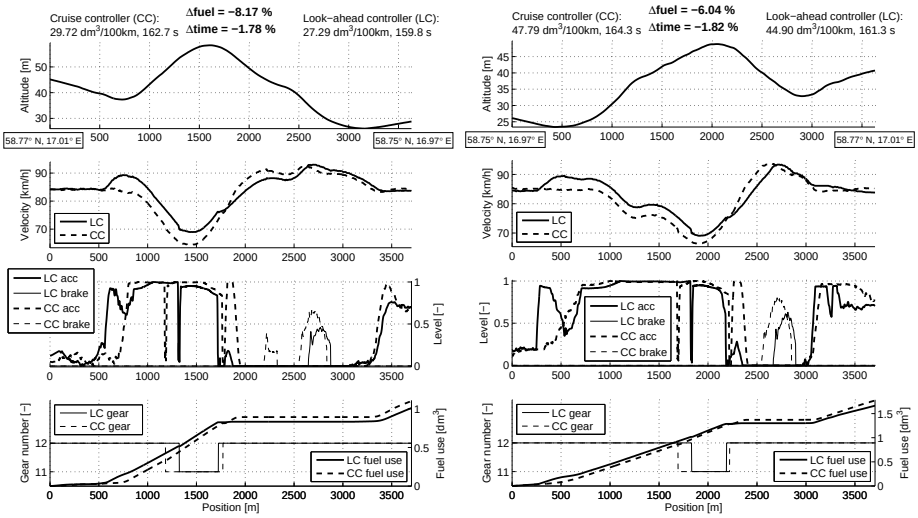

Figure 8.3: The Hållet segment. Left: The LC accelerates at 500 m prior to the uphill and slows down at 1750 m when the top is reached. Right: Similar characteristics, an acceleration at 250 m and a slow-down at 2250 m.

The Järna Segment

In Figure 8.4, the Järna segment is shown. The matching simulation is shown in Figure 7.6 (p. 61). The left figure shows that the LC begins to gain speed at 200 m and slows down at 1400 m. This agrees well with the simulated behavior. In the measurements, the LC avoids the gear shift that the CC is forced to do around 1 km while there are no gear shifts in the simulation. The reason is likely the fact that the simulated velocity near the top of the hill is slightly less than measured.

In the right half of Figure 8.4 and Figure 7.6 a drive in the other direction is shown. In the experiment, the LC accelerates at 500 m and starts to slow

down at 1400 m. The slow-down lessen the braking effort needed at about 2000 m. The acceleration at 500 m do not appear in the simulated drive and here clear differences arise compared to the experiment. The cause of this will be investigated further in the following section.

The absolute values of fuel use differ, especially for the road segment to the left in the figures. A comparison in the other direction is not justified since the velocity trajectories are so different.

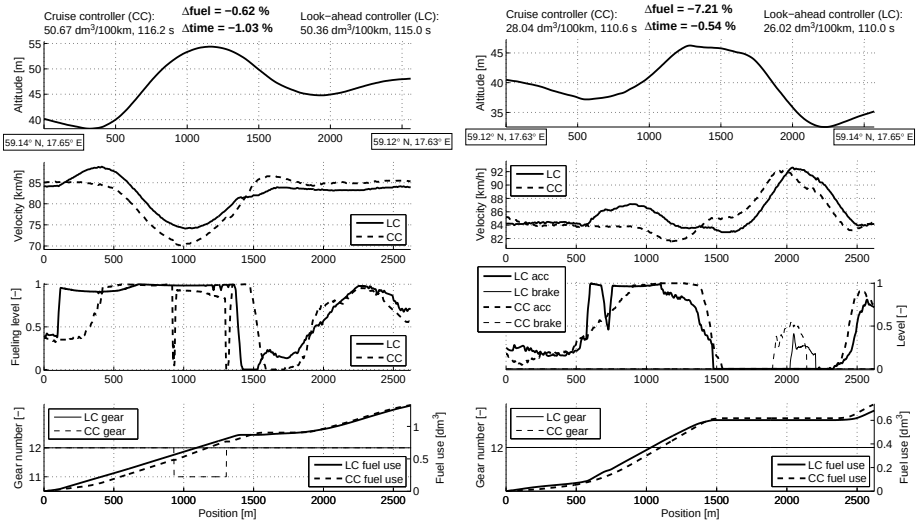

Figure 8.4: The Järna segment. Left: The LC gains speed at 200 m prior to the uphill and avoids a gear shift. At 1400 m the LC slows down and the truck is let to accelerate in the downslope. Right: The LC accelerates at 500 m and slows down at 1400 m thereby reducing the braking effort needed later on.

8.1.3 Rolling Horizon

To further study properties of look-ahead control, the solution trajectories obtained in each iteration are compared to the set point sent to the cruise controller and the resulting velocity. The road segments studied earlier will be examined. This will reveal some effects of feedback to the look-ahead controller and also aid in explaining some of the observed behavior of the controller characteristics. The road segments used are the Järna and the Hållet segments studied earlier and the Stavsjö segment, see Section 6.5.1.

The look-ahead control strategy repeatedly solves an optimization problem online by using a truncated horizon, see Section 2.4 and Figure 2.2, that with current parameters is 1500 m. In each iteration, a control and state sequence is found that minimizes a criterion. The velocity trajectory of the solution is studied here.

The trajectories were obtained offline by applying the algorithm every 50 m with the initial values given by the recorded data and using the same road data. Each figure is divided into two both having position as the horizontal axis, see e.g. Figure 8.5. The top part shows the road topography and the bottom part shows the velocity trajectories. The solution trajectories are drawn with solid thin lines in the figures. The measured velocity is drawn with a thick solid line and the measured set point that was fed to the cruise controller is drawn with a thin dashed line.

The Hållet Segment

Figure 8.5 shows the Hållet segment. The corresponding controller characteristics are shown in Figure 8.3. In the left half of the figure the trajectories are rather agreeing. A spread appears at about the top of the hill at 1500 m where many solution trajectories lies above the measured. Between 2.5 km and 3 km, all solutions stays at 89 km/h which was the upper bound in the optimization interval.

In the right half of Figure 8.5, the trajectories are not as agreeing as in the other direction. Between 250 m and 500 m it is seen that the solution trajectories start with a velocity clearly higher than the previous trajectory for at least three samples. In the beginning, the actual acceleration thus seems to be larger than predicted. On the other hand, the deceleration at the top of the hill seems larger than predicted and thus causing a spread among the trajectories. The road segment in Figure 8.5 is the same as in Figure 7.2 in Section 7.1 where a comparison between measured and predicted data suggests that the slope is crudely estimated in this particular road segment. Figure 8.5 indicates that the slope at the beginning and around the top of the hill at about 2 km might be underestimated which would explain the spread of the trajectories. If for example the estimated vehicle mass was the main source of these errors, the errors would be agreeing. At first the errors are equivalent to an estimated mass higher than in reality and later the situation is the opposite. A certain conclusion, though, can not be drawn from these data.

The segment around 2 km in Figure 8.5 reveals some effects of feedback to the look-ahead controller. Since the initial velocity is fed to the algorithm every trajectory should start out reasonable accurately. But if the slope is underestimated, the solution trajectories will continue to lie above the one that will actually result if it is not possible for the inner loop to realize the solution trajectory.

The Järna Segment

Figure 8.6 shows the Järna segment. The matching controller characteristics are shown in Figure 8.4. In the left half of the figure, the trajectories are rather consistent with the exception for an interval around 1 km.

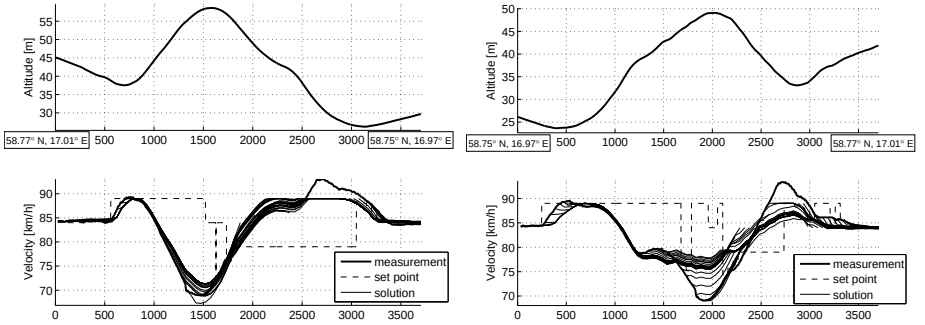

Figure 8.5: The Hållet segment. Left: Consistent solution trajectories. Right: A spread of the trajectories in the beginning and the second half of the section.

In the right half of Figure 8.6, the road segment is shown in the other direction. The trajectories have a large spread from 500 m to the end of the segment. At about 500 m, it shows that the solution trajectories do not entail an acceleration prior to the uphill in the middle of the segment. The control rules do however wrongly interpret the solution as an acceleration and adjust the set point accordingly. In the downhill the acceleration is clearly underestimated. The resulting trip time and fuel use are however satisfactory in comparison with the cruise controller, see Figure 8.4. A possible downside is the perception of the ride due to the fact that the set point makes a large step for one sample at about 700 m causing the acceleration to cease for that sample. However, the sole source of this behavior is the mentioned problem with tracking characteristics that should be made obsolete by another configuration of the inner control loop that is, the cruise controller.

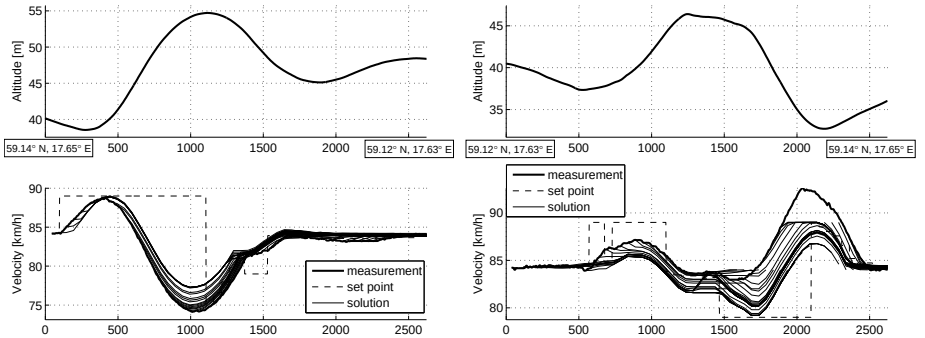

Figure 8.6: The Järna segment. Left: The trajectories are consistent besides around 1 km. Right: A large spread of the trajectories in most of the section. The control rule increases the set point at 500 m and that gives an actual trajectory different than the solution trajectories.

The Stavsjö Segment

In Figure 8.7 the Stavsjö segment is shown. This road segment is chosen to illustrate how the rolling horizon influences the solution trajectories. The look-ahead horizon is 1500 m and the downhill is therefore not visible for the controller in the beginning of the segment. The more of the downhill that is covered by the horizon, the greater the deceleration prior the downhill becomes. This lead to a gradual decrease of the set point at first until at about 1200 m when the control rule decides to set the lowest possible set point value of 79 km/h.

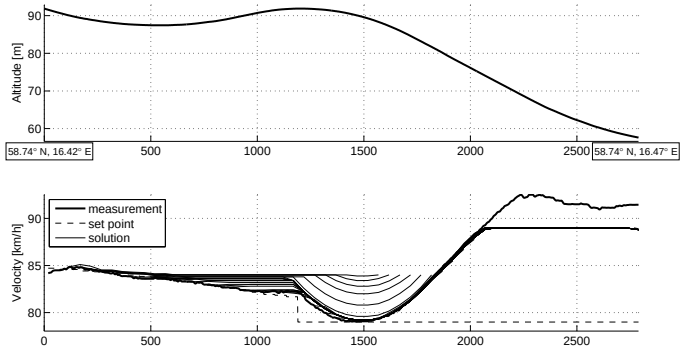

Figure 8.7: The Stavsjö segment. The slow-down prior to the downhill becomes more evident as the vehicle and the look-ahead horizon proceeds.

8.2 Conclusions

A fuel consumption reduction of about 3.5% on the 120 km route without an increase in trip time was obtained in the experiments. The mean number of gear shifts was reduced with 42% due to shifts avoided by gaining speed prior to uphills. The look-ahead control mainly differs from conventional cruise control near significant downhills and uphills where the look-ahead control in general slows down or gains speed prior to the hill. Slowing down prior to downhills is intuitively saving fuel, and accelerating prior to uphills is one way which, at least for shorter hills, gives a higher velocity throughout the hill and will reduce the need for lower gears. The crucial problem is really how and when to effectuate these control actions. This depends non-trivially on the vehicle and the road, e.g. the mass and road slope, and the algorithm handles this well.

By comparing simulations with the experiments, it was seen that the overall impact of look-ahead control on the performance measures are well predicted. Further, the controller characteristics were studied in more detail on selected interesting road segments. The behavior was captured relative to simulations, and thus giving validating evidence of both model and algorithm in real experiments.

9

Conclusions

A look-ahead control strategy has been developed with the aim to reduce the fuel consumption of a heavy truck by utilizing information about the road topography ahead. The strategy repeatedly solves a discretized and truncated problem online by means of a tailored dynamic programming algorithm.

The mass is the most important parameter in the current context. The vehicle mass of a heavy truck is tens of tonnes. Due to the large mass even moderate slopes become significant. Therefore it is in general not possible to keep a desired cruising speed, the velocity will inevitably vary. Further, the loss of propulsion force when shifting gear has a noteworthy influence on vehicle motion. A prediction model taking these effects into account is of hybrid nature and includes time delays. The large vehicle mass thus causes a challenging optimization problem.

The optimization algorithm gives satisfactory solutions with a sufficiently low computational complexity. A key step was to avoid problems due to numerical errors. The final algorithm computes a solution in tenths of a second on a modern laptop computer and this allowed realization in a demonstrator vehicle and experimental evaluation.

The prediction model was demonstrated to capture the dynamics due to control and road topography. The simulation environment predicted the performance of the look-ahead controller close to the actual values measured in real trial runs. The validation of the models for prediction and evaluation forms a reliable base for algorithm development. It also reinforces the current experimental results by showing how the potential of the control vary with a number of parameters.

Experiments were performed on a 120 km segment on a Swedish highway with moderate slopes. The demonstrator showed about 3.5% reduction of the fuel consumption without an increase in the travel time back and forth on this route. Further, the number of gearshifts was notably reduced. The typical characteristics of the velocity trajectories obtained with look-ahead control are intuitive. The crucial issue is the detailed shape of the solution and its actuation such that a positive end result is obtained, and this is shown to be handled well by the algorithm. Finally, the controller behavior has been perceived as comfortable and natural by drivers and passengers that have participated in tests and demonstrations.

References

Back, M. (2006). *Prädiktive Antriebsregelung zum energieoptimalen Betrieb von Hybridfahrzeugen*. PhD thesis, Universität Karlsruhe, Karlsruhe, Germany.

Back, M., Simons, M., Kirschaum, F., and Krebs, V. (2002). Predictive control of drivetrains. IFAC World Congress, Barcelona, Spain.

Back, M., Terwen, S., and Krebs, V. (2004). Predictive powertrain control for hybrid electric vehicles. 4th IFAC Symposium on Advances in Automotive Control, Salerno, Italy.

Bellman, R. (1957). *Dynamic Programming*. Princeton University Press, Princeton, New Jersey.

Bellman, R. (1961). *Adaptive Control Processes: A Guided Tour*. Princeton University Press, Princeton, New Jersey.

Bellman, R. and Dreyfus, S. (1962). *Applied Dynamic Programming*. Princeton University Press, Princeton, New Jersey.

Bemporad, A. and Morari, M. (1999). Control of systems integrating logic, dynamics and constraints. *Automatica*, 35(3):407–427.

Bertsekas, D. (1995). *Dynamic Programming and Optimal Control*, volume I. Athena Scientific, Belmont, Massachusetts.

Bertsekas, D. P. (2005). Dynamic programming and suboptimal control: A survey from ADP to MPC. *European Journal of Control*, 11.

Borrelli, F., Bemporad, A., Fodor, M., and Hrovat, D. (2006). An MPC/hybrid system approach to traction control. *IEEE Trans. Contr. Systems Technology*, 14(3):541–552.

Camacho, E. and Bordons, C. (2004). *Model Predictive Control*. Springer-Verlag, London.

Chang, D. J. and Morlok, E. K. (2005). Vehicle speed profiles to minimize work and fuel consumption. *Journal of transportation engineering*, 131(3):173–181.

Denardo, E. (1982). *Dynamic Programming: models and applications*. Prentice-Hall, Englewood Cliffs, New Jersey.

Eriksson, L., Fredriksson, J., Fröberg, A., Krus, P., Larsson, J., Nielsen, L., and Sjöberg, J. (2004). Center for automotive propulsion simulation. http://www.capsim.se/.

Finkeldei, E. and Back, M. (2004). Implementing an MPC algorithm in a vehicle with a hybrid powertrain using telematics as a sensor for powertrain control. 4th IFAC Symposium on Advances in Automotive Control, Salerno, Italy.

Fröberg, A., Hellström, E., and Nielsen, L. (2006). Explicit fuel optimal speed profiles for heavy trucks on a set of topographic road profiles. Number 2006-01-1071 in SAE World Congress, Detroit, MI, USA.

Fröberg, A. and Nielsen, L. (2007). Optimal fuel and gear ratio control for heavy trucks with piece wise affine engine characteristics. 5th IFAC Symposium on Advances in Automotive Control, Monterey, CA, USA.

Fröberg, A., Nielsen, L., Hedström, L.-G., and Pettersson, M. (2005). Controlling gear engagement and disengagement on heavy trucks for minimization of fuel consumption. IFAC World Congress, Prague, Czech Republic.

Gelfand, I. and Fomin, S. (1963). *Calculus of variations*. Prentice-Hall, Englewood Cliffs, New Jersey.

Gillespie, T. (1992). *Fundamentals of vehicle dynamics*. Society of Automotive Engineers, Warrendale, Pennsylvania.

Giorgetti, N., Bemporad, A., Tseng, H. E., and Hrovat, D. (2006a). Hybrid model predictive control application towards optimal semi-active suspension. *International Journal of Control*, 79(5):521–533.

Giorgetti, N., Ripaccioli, G., Bemporad, A., Kolmanovsky, I., and Hrovat, D. (2006b). Hybrid model predictive control of direct injection stratified charge engines. *IEEE/ASME Transactions on Mechatronics*, 11(5):499–506.

Guzzella, L. and Sciarretta, A. (2005). *Vehicle Propulsion Systems - Introduction to Modeling and Optimization*. Springer-Verlag, Berlin.

Hellström, E., Fröberg, A., and Nielsen, L. (2006). A real-time fuel-optimal cruise controller for heavy trucks using road topography information. Number 2006-01-0008 in SAE World Congress, Detroit, MI, USA.

Hellström, E., Ivarsson, M., Åslund, J., and Nielsen, L. (2007). Look-ahead control for heavy trucks to minimize trip time and fuel consumption. 5th IFAC Symposium on Advances in Automotive Control, Monterey, CA, USA.

Hooker, J. (1988). Optimal driving for single-vehicle fuel economy. *Transportation Research*, 22A(3):183–201.

Hooker, J., Rose, A., and Roberts, G. (1983). Optimal control of automobiles for fuel economy. *Transportation Science*, 17(2):146–167.

Howlett, P. (1996). Optimal strategies for the control of a train. *Automatica*, 32(4):519–532.

IEEE Standards Board (1985). IEEE standard for binary floating-point arithmetic. IEEE Std 754-1985.

Jonsson, J. and Jansson, Z. (2004). Fuel optimized predictive following in low speed conditions. 4th IFAC Symposium on Advances in Automotive Control, Salerno, Italy.

Kiencke, U. and Nielsen, L. (2005). *Automotive Control Systems, For Engine, Driveline, and Vehicle*. Springer-Verlag, Berlin, 2nd edition.

Kirschbaum, F., Back, M., and Hart, M. (2002). Determination of the fuel-optimal trajectory for a vehicle along a known route. IFAC World Congress, Barcelona, Spain.

Lagerberg, A. and Egardt, B. (2007). Backlash estimation with application to automotive powertrains. *IEEE Transactions on Control Systems Technology*, 15(3):483–493.

Larson, R. and Casti, J. (1978). *Principles of Dynamic Programming*. Marcel Dekker, Madison Avenue, New York.

Lattemann, F., Neiss, K., Terwen, S., and Connolly, T. (2004). The predictive cruise control - a system to reduce fuel consumption of heavy duty trucks. SAE Technical paper series 2004-01-2616.

Levine, W. S. (1996). *The Control Handbook*. CRC Press and IEEE Press.

Liu, R. and Golovitcher, I. (2003). Energy-efficient operation of rail vehicles. *Transportation Research*, 37A:917–932.

Monastyrsky, V. and Golownykh, I. (1993). Rapid computations of optimal control for vehicles. *Transportation Research*, 27B(3):219–227.

Neiss, K., Terwen, S., and Connolly, T. (2004). Predictive speed control for a motor vehicle. United States Patent Application Publication 2004/0068359.

Pacejka, H. B. (2002). *Tyre and Vehicle Dynamics*. Elsevier, Oxford.

Pettersson, M. (1997). *Driveline Modeling and Control*. PhD thesis, Linköping University, Linköping, Sweden.

Pettersson, M. and Nielsen, L. (2000). Gear shifting by engine control. *IEEE Transactions on Control Systems Technology*, 8(3):495–507.

Pettersson, N. and Johansson, K. (2004). Modelling and control of auxiliary loads in heavy vehicles. *International Journal of Control*, 79(5):479–495.

Sahlholm, P., Jansson, H., Kozica, E., and Johansson, K. (2007). A sensor and data fusion algorithm for road grade estimation. 5th IFAC Symposium on Advances in Automotive Control, Monterey, CA, USA.

Sandberg, T. (2001a). Heavy truck modeling for fuel consumption: Simulations and measurements. Technical report, Linköping University. LiU-TEK-LIC-2001:61, Thesis No. 924.

Sandberg, T. (2001b). Simulation tool for predicting fuel consumption for heavy trucks. IFAC Workshop: Advances in Automotive Control, Karlsruhe, Germany.

Schittler, M. (2003). State-of-the-art and emerging truck engine technologies for optimized performance, emissions, and life-cycle costing. 9th Diesel Engine Emissions Reduction Conference, Rhode Island, USA. U.S. Department of Energy.

Schwarzkopf, A. and Leipnik, R. (1977). Control of highway vehicles for minimum fuel consumption over varying terrain. *Transportation Research*, 11(4):279–286.

Terwen, S., Back, M., and Krebs, V. (2004). Predictive powertrain control for heavy duty trucks. 4th IFAC Symposium on Advances in Automotive Control, Salerno, Italy.

Volvo press release (2006). Volvo delivers I-shift automated transmission for North America. http://www.volvo.com/.

Wong, J. (2001). *Theory of Ground Vehicles*. John Wiley, New York.